

Global Panel of HIV-1 Env Reference Strains for Standardized Assessments of Vaccine-Elicited Neutralizing Antibodies

Allan deCamp,^a Peter Hrabec,^b Robert T. Bailer,^c Michael S. Seaman,^d Christina Ochsenbauer,^e John Kappes,^{e,f} Raphael Gottardo,^a Paul Edlefsen,^a Steve Self,^a Haili Tang,^g Kelli Greene,^g Hongmei Gao,^g Xiaoju Daniell,^g Marcella Sarzotti-Kelsoe,^{g,h} Miroslaw K. Gorny,ⁱ Susan Zolla-Pazner,^{ij} Celia C. LaBranche,^g John R. Mascola,^c Bette T. Korber,^b David C. Montefiori^g

Fred Hutchinson Cancer Research Center, Seattle, Washington, USA^a; Theoretical Biology and Biophysics, Los Alamos National Laboratory, Los Alamos, New Mexico, USA^b; Vaccine Research Center, National Institute of Allergy and Infectious Diseases, National Institutes of Health, Bethesda, Maryland, USA^c; Center for Virology and Vaccine Research, Beth Israel Deaconess Medical Center, Harvard Medical School, Boston, Massachusetts, USA^d; University of Alabama at Birmingham, Birmingham, Alabama, USA^e; Birmingham Veterans Affairs Medical Center, Research Service, Birmingham, Alabama, USA^f; Departments of Surgery^g and Immunology,^h Duke University Medical Center, Durham, North Carolina, USA; Department of Pathology, New York University Langone School of Medicine, New York, New York, USAⁱ; Research Center for AIDS and HIV Infection, Veterans Affairs Medical Center, New York, New York, USA^j

ABSTRACT

Standardized assessments of HIV-1 vaccine-elicited neutralizing antibody responses are complicated by the genetic and antigenic variability of the viral envelope glycoproteins (Envs). To address these issues, suitable reference strains are needed that are representative of the global epidemic. Several panels have been recommended previously, but no clear answers have been available on how many and which strains are best suited for this purpose. We used a statistical model selection method to identify a global panel of reference Env clones from among 219 Env-pseudotyped viruses assayed in TZM-bl cells with sera from 205 HIV-1-infected individuals. The Envs and sera were sampled globally from diverse geographic locations and represented all major genetic subtypes and circulating recombinant forms of the virus. Assays with a panel size of only nine viruses adequately represented the spectrum of HIV-1 serum neutralizing activity seen with the larger panel of 219 viruses. An optimal panel of nine viruses was selected and augmented with three additional viruses for greater genetic and antigenic coverage. The spectrum of HIV-1 serum neutralizing activity seen with the final 12-virus panel closely approximated the activity seen with subtype-matched viruses. Moreover, the final panel was highly sensitive for detection of many of the known broadly neutralizing antibodies. For broader assay applications, all 12 Env clones were converted to infectious molecular clones using a proviral backbone carrying a *Renilla* luciferase reporter gene (Env.IMC.LucR viruses). This global panel should facilitate highly standardized assessments of vaccine-elicited neutralizing antibodies across multiple HIV-1 vaccine platforms in different parts of the world.

IMPORTANCE

An effective HIV-1 vaccine will need to overcome the extraordinary genetic variability of the virus, where most variation occurs in the viral envelope glycoproteins that are the sole targets for neutralizing antibodies. Efforts to elicit broadly cross-reactive neutralizing antibodies that will protect against infection by most circulating strains of the virus are guided in part by *in vitro* assays that determine the ability of vaccine-elicited antibodies to neutralize genetically diverse HIV-1 variants. Until now, little information was available on how many and which strains of the virus are best suited for this purpose. We applied robust statistical methods to evaluate a large neutralization data set and identified a small panel of viruses that are a good representation of the global epidemic. The neutralization properties of this new panel of reference strains should facilitate the development of an effective HIV-1 vaccine.

Assessments of HIV-1 vaccine-elicited neutralizing antibody (nAb) responses need to adequately address the multiple genetic subtypes and neutralization phenotypes of the virus (1). Genetic variability has given rise to at least nine genetic subtypes and a growing number of circulating recombinant forms (CRFs), where >90% of the current epidemic is driven by subtypes A, B, C, D, G, CRF01, and CRF02 (2) and where the prevalence of each subtype and CRF fluctuates geographically (3). HIV-1 variants also exhibit a wide range of neutralization susceptibilities with sera from chronically infected individuals (4). A small subset of circulating and passaged variants exhibits extraordinary sensitivity that is classified as a tier 1 phenotype. Variants with this phenotype exhibit spontaneous exposure of highly immunogenic epitopes in the variable loops and coreceptor binding domain of gp120 (5–7). These epitopes are poorly exposed on most circulating strains, resulting in an overall lower level of neutralization susceptibility that is classified as a tier 2 phenotype. Another small fraction of

circulating variants is even less sensitive to neutralization and classified as having a tier 3 phenotype. Tier 2 variants, being most abundant in the epidemic, are given the highest priority to target with vaccines (1, 8, 9).

Despite poor exposure of some epitopes on the surface gp120 and transmembrane gp41 envelope glycoproteins (Envs) of tier 2 and 3 HIV-1 variants, several regions are vulnerable to nAbs; these

Received 29 September 2013 Accepted 14 November 2013

Published ahead of print 18 December 2013

Editor: B. H. Hahn

Address correspondence to David C. Montefiori, monte@duke.edu.

Copyright © 2014, American Society for Microbiology. All Rights Reserved.

doi:10.1128/JVI.02853-13

include epitopes in the CD4 binding site (CD4bs), V1V2 glycan, V3/V4 glycan, and glycan-exclusive regions of gp120, as well as several epitopes in the membrane proximal external region (MPER) of gp41 (10–13). Other sites of vulnerability may exist that have yet to be identified. These vulnerabilities afford a number of opportunities for vaccines to elicit antibodies that neutralize most circulating strains of HIV-1. Various strategies are under investigation to induce such responses. Some strategies take a structure-based approach that aims to mimic broadly neutralizing epitopes on native functional Env spikes (14, 15). Recent examples include the optimization and stabilization of epitopes in the receptor and coreceptor binding regions of gp120 (16–19), the design of innovative structural variants of gp41 (20–22), and the design of optimal mimics of gp120 and gp41 epitopes recognized by broadly neutralizing Abs (bnAbs) (23–26). Other approaches focus on B regulation, such as self-tolerance (27, 28) and suspected immunosuppressive properties of gp120 (29–31). Another recent approach is the recruitment of germ line and intermediate B cell precursors involved in the production of bnAbs (32–34). As new vaccine concepts enter preclinical and clinical phases of testing, it will be important to compare the magnitudes and breadths of nAb responses using a relevant spectrum of HIV-1 variants that are representative of the global epidemic.

Several panels of molecularly cloned HIV-1 Env variants have been recommended for use as reference strains. These panels are comprised of multiple subtypes and were selected to be genetically and antigenically diverse. Subtype B and C tier 2 panels were proposed (35, 36), based on viruses that were not unusually sensitive or resistant to neutralization by HIV-1-positive plasma samples, while maintaining specificities that resemble the known bnAbs at that time (e.g., IgG1b12, 2G12, 2F5, and 4E10). The mode of transmission and diversity, both genetic and geographic, were also considered. A panel size of 12 was recommended based on sample size calculations (37), but the ideal size and composition of reference panels have remained uncertain. Initial reference panels for subtypes B (35) and C (36) were based on 12 strains selected from among 18 or 19 candidate strains studied. Although it was an important step to identify initial reference panels for these two major circulating subtypes, the panels were selected from a relatively small number of candidate strains. Moreover, the criteria used for selection were largely subjective.

Brown et al. (38) studied a panel of 60 uncloned primary isolates, comprising 10 isolates from each of the six major subtypes. They recommended that the panel be used as a resource for measuring cross-clade nAbs when comparing different vaccines using neutralization assays in peripheral blood mononuclear cells (PBMC). Moreover, Simek et al. (39) identified a set of seven Env-pseudotyped viruses from among a multisubtype panel of 35 Env-pseudotyped viruses with the greatest utility for identification of sera with potent broadly neutralizing activity. Their goal was to identify elite neutralizers for the isolation of novel bnAbs. In their study, samples identified as having titers of ≥ 100 (Env-pseudotyped viruses assayed in U87.CD4.CCR5 cells) to at least four of five subtypes consistently had breadth within and across subtypes to larger panels. Their results also suggested that samples with neutralizing activity against multiple subtype B viruses also tended to neutralize multiple subtype C viruses. They concluded that neutralizing activity against multiple genetic subtypes from multiple geographic regions can be reliably assessed using a small panel of viruses. They found no difference in neutralization pat-

terns among viruses isolated during chronic and acute infection. They suggest that neutralization screening panels need not take into account Fiebig stage and time of collection but should instead focus on the overall neutralization phenotype of the virus to serum samples and monoclonal antibodies (MAbs).

A single, reasonably sized panel of HIV-1 reference strains that adequately reflects the global epidemic regardless of subtype would facilitate comparisons across studies and would especially benefit vaccine development, which relies heavily on comparative immunogenicity data. We describe a systematic method based on a statistical model selection procedure known as “lasso” to identify a global panel of nine reference Env clones from among 219 Env-pseudotyped viruses based on the spectrum of neutralizing activity seen with sera from 205 chronically HIV-1-infected individuals, where both the Envs and sera were sampled globally and represented all major genetic subtypes and CRFs of the virus.

MATERIALS AND METHODS

Serum samples and MAbs. After obtaining written informed consent, serum samples were obtained from 205 chronically infected individuals who were antiretroviral drug-naïve and infected with HIV-1 subtypes A ($n = 8$), B ($n = 59$), C ($n = 58$), D ($n = 3$), CRF01_AE ($n = 15$), CRF07_BC ($n = 16$), CRF02_AG ($n = 2$), CRF10_CD ($n = 1$), AC ($n = 4$), AD ($n = 3$), and ABCD ($n = 2$); 34 were infected with subtypes that could not be determined due to low levels of plasma viremia. HIV-1 genetic subtypes were determined by single-genome amplification and sequencing of a single serum gp160 gene as described previously (35). Conserved nAb epitopes were probed with the CD4bs bnAbs VRC01 (40, 41), VRC-CH31 (42, 43), HJ16 (44), and IgG1b12 (45), the V1V2 glycan-specific bnAbs PG9, PG16 (46), and CH01 (42, 47), the V3/V4 glycan bnAb PGT128 (48), the gp120 glycan-specific bnAb 2G12 (49), and the gp41 MPER bnAbs 2F5 and 4E10 (50). Other neutralization epitopes were probed with CD4bs MAbs 654-30D (51), 1008-30D, 1570D (52), and 729-30D (53), the V3-specific MAbs 2219 (54), 2557 (55), 3074 (56), 3869 (57), 447-52D, 412D (58), and 838-D (59), the V2-specific MAbs 1361, 1357D (60), 1393A, 830A (61), 697-30D (62), and 2297 (63), the C2-specific MAb 847D (61), the C5-specific MAbs 1331-160A (60), 670-30D, and 858-30D (53), the gp41 cluster I-specific MAbs 181D, 246D, 240D (64), 50-69D (65), and 4B3 (unpublished), the gp41 cluster II-specific MAbs 126-7D and 167D (64), and MAbs 17b and E51 to CD4-induced (CD4i) epitopes on gp120 (36). The MAbs 1418 (66) and 3685A (unpublished) to parvovirus b19 and anthrax protective antigen (PA), respectively, were used as negative controls.

Env-pseudotyped viruses. Functional full-length *rev-env* cassettes for making Env-pseudotyped viruses were cloned by single-genome amplification from plasma viral RNA as described previously (35, 36) from 219 subjects infected with HIV-1 subtypes A ($n = 10$), B ($n = 54$), C ($n = 67$), D ($n = 5$), G ($n = 8$), CRF01_AE ($n = 21$), CRF02_AG ($n = 16$), CRF06 ($n = 1$), CRF07_BC ($n = 14$), AC ($n = 6$), AD ($n = 5$), ACD ($n = 1$), BC ($n = 4$), BG ($n = 1$), and CD ($n = 6$). Where available, Fiebig stages were noted. Because Fiebig stages were frequently unknown or ranged in value, we defined three infection stage categories: early (Fiebig stages I to IV), intermediate (Fiebig stages V to early VI), and late (late Fiebig stage VI, 6 or more months postinfection through chronic), where known.

Env.IMC.LucR viruses. *env* sequences from the 12 *rev-env* cassettes selected as global reference reagents were cloned into otherwise isogenic, replication-competent infectious molecular clones carrying a Tat-regulated *Renilla* Luc reporter gene (Env.IMC.LucR viruses) as described previously (67). Unless otherwise indicated, all Env.IMC.LucR viruses contained the entire ectodomain of the Env of choice fused to the transmembrane and cytoplasmic tail regions of NL4-3 (67). A parallel set of viruses (Env.IMC.LucR.RE) was generated carrying the respective entire *rev-env* cassettes of the 12 reference strains as described elsewhere (C. Ochsenbauer and J. Kappes, unpublished data).

Analysis coreceptor tropism. Coreceptor usage of the newly identified global reference panel of Env-pseudotyped viruses and their corresponding Env-IMC.LucR viruses was assessed in TZM-bl and A3R5 cells, respectively, by assaying multiple concentrations of the R5 inhibitor TAK-779 and the X4 inhibitor AMD 3100 as described below for neutralization assays. Both reagents were obtained from the NIH AIDS Reagent Program, as contributed by the Division of AIDS, NIH (Bethesda, MD).

Neutralization assays. Neutralization of Env-pseudotyped viruses was measured in 96-well culture plates by using Tat-regulated firefly luciferase (Luc) reporter gene expression to quantify reductions in virus infection in TZM-bl cells (68). Neutralization of Env-IMC.LucR viruses was similarly measured by using Tat-regulated *Renilla* Luc reporter gene expression in A3R5 cells (69). Both assays have been formally optimized and validated (70, 71). Heat-inactivated (56°C, 1 h) serum samples were assayed at 3-fold dilutions starting at 1:20. Neutralization titers (50% inhibitory dose [ID₅₀]) are the serum dilution at which relative luminescence units (RLU) were reduced by 50% compared to RLU in virus control wells after subtraction of background RLU in cell control wells. Neutralizing activity also was measured as a function of the area under the positive portion of the neutralization curve (pAUC); here, values less than 0% neutralization due to normal variation of the assay or mild infection enhancement at high serum dilutions were not used. As described below, pAUC values were used for statistical analyses, whereas ID₅₀ values were used for more conventional descriptions of virus phenotypes. Assay stocks of Env-pseudotyped viruses and Env-IMC.LucR viruses were produced by transfection in 293T cells and titrated in either TZM-bl or A3R5 cells as described previously (67, 68).

Neutralization scores. While the ID₅₀ is one summary measure of a dilution series used to represent nAb titers, it results in a loss of information at low neutralization potencies that do not reach 50% at the lowest serum dilution tested. We have found that using pAUC is a more general and useful way to summarize nAb activity for statistical analyses, since it is more sensitive at low neutralization potencies and correlates with positive ID₅₀ values (72). To evaluate aggregate neutralization behavior across viruses, for any serum sample, nAb titer and breadth across a panel of isolates were represented together by a magnitude-breadth (MB) curve, which is a cumulative distribution function that represents the proportion of isolates neutralized with potency no less than x for every point along the x axis (73). We computed three neutralization scores per serum to quantify MB curves: quartiles of the MB curve Q_1 , Q_2 , and Q_3 , defined as the potency values corresponding to breadths of 75, 50, and 25%, respectively, of the cumulative distribution of neutralization values across all viruses. We also computed average serum potency across a set of isolates, or the area under the MB curve (AUC-MB), to determine optimal panel sizes.

Panel selection. Lasso is the constrained regression procedure used to select isolate combinations that best predicted neutralization scores. Briefly, lasso uses penalized regression to minimize error, with a constraint on the sum of the absolute values of regression coefficients (74). This constraint makes most terms of the regression model vanish, leaving a small fixed number of isolates that predict neutralization. Each neutralization score defines a distinct panel selection method based on the selected isolates. We used panels consisting of K isolates (K ranging between 1 and 20) selected by lasso to predict neutralization scores for each serum by using hard thresholding, which models neutralization scores with coefficients from ordinary (unconstrained) linear regression. We also evaluated a multivariate combination of quartiles Q_1 , Q_2 , and Q_3 using grouped lasso (75), although for brevity, the results are not shown.

Prediction of serum MB curves. Subsets of viruses were sought whose performance with serum samples predicted the actual performance of the samples against the larger set of viruses. Consistent sigmoidal shapes of MB curves across sera, corresponding to near Gaussian neutralization response distributions, simplified the problem of modeling the neutralization distribution per serum. Predicted MB curves were determined with subsets of viruses by fitting a logistic function (76) to quartiles of the distribution, using the R package *drc* for parameter estimates (77). We

measured the fit of a predicted MB curve to the observed MB curve using the area between these two curves (ABC) from 0 to 1 (i.e., the average distance between the curves). We also computed an R^2 value from the area under the predicted and observed MB curves. The R^2 for AUC-MB is defined across M sera as

$$1 - \frac{\sum_{j=1}^m (A_j - \hat{A}_j)^2}{\sum_{j=1}^m (A_j - \bar{A})^2}$$

where A_j is the observed AUC-MB curve for serum j across all viruses, \hat{A}_j is the predicted AUC-MB for serum j across all viruses, and \bar{A} is the average of the observed AUC-MB curves. The global panel analysis used 205 sera and 195 virus isolates with all observations present, rather than accommodate missing data.

Subtype-specific panels. We were also interested in generating subtype-specific prediction panels. For subtypes B and C, we had enough type-specific sera and isolates to consider subtype-specific panels. For subtype B, we used 59 sera and 49 isolates, and for subtype C (including subtype CRF07, which is almost entirely a C clade virus in the Env region) we used 74 sera and 75 isolates. The non-B/non-C data consisted of 72 sera and 71 isolates, although noncirculating recombinants included various fragments of B and C.

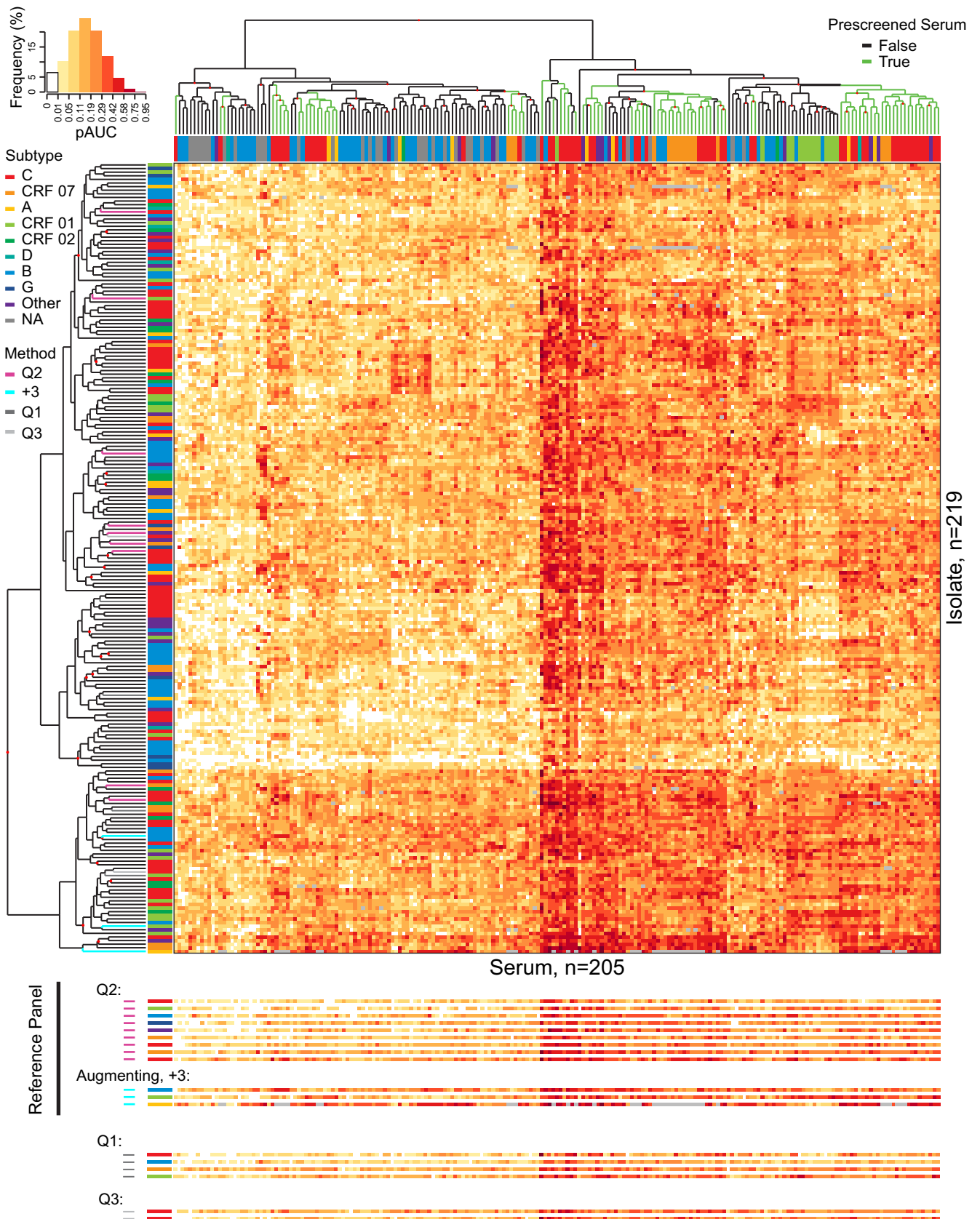
Performance evaluation. To assess panel selection performance, we compared lasso-selected and randomly chosen panels. For each candidate panel size, we randomly sampled 1,000 panels of that size, used ordinary linear regression to predict the AUC-MB from each, and compared the results using the coefficient of determination, R^2 , from linear regression. Independent performance assessment requires that data used to estimate parameters be excluded from data used to assess accuracy. Therefore, we also used 10-fold cross-validation to assess performance of quartile-based prediction methods. We split sera into 10 groups of 20 or 21 sera, and then for each group performed panel selection using sera not in that group to compute the ABC per serum in the group.

For subtype-specific panels, we computed ABC between predicted and observed MB curves using clade-matched data. We added isolates from the global panel, using the additional data to predict subtype-specific MB curves (i.e., MB curves restricted to isolates of a given HIV-1 subtype). We compared ABCs of subtype-specific and global panels to evaluate subtype-specific panels and evaluated the performance of previously defined panels for subtypes B and C (35, 36) to predict serum MB curves. Since previously defined panels included isolates not among the 195 viruses used to define the global panel, we used a matrix of 164 sera (55 subtype B, 38 subtype C, 71 non-B/non-C) by 165 viruses (37 subtype B, 61 subtype C, 67 non-B/non-C) when assessing these panels with complete data.

RESULTS

Global reference panel selection. The neutralization profile of 219 HIV-1 Env-pseudotyped viruses was assessed in a checkerboard style in TZM-bl cells with serum samples from 205 chronically HIV-1-infected subjects. Env pseudotypes originated in Kenya ($n = 7$), Uganda ($n = 10$), Rwanda ($n = 1$), Tanzania ($n = 28$), the United States ($n = 30$), Italy ($n = 2$), Trinidad/Tobago ($n = 6$), Thailand ($n = 29$), Spain ($n = 7$), Peru ($n = 8$), China ($n = 35$), India ($n = 9$), South Africa ($n = 13$), Zambia ($n = 9$), Malawi ($n = 16$), Brazil ($n = 1$), Ghana ($n = 1$), Senegal ($n = 5$), Portugal ($n = 1$), and Switzerland ($n = 1$). Serum samples originated in China ($n = 20$), Europe ($n = 16$), Malawi ($n = 9$), South Africa ($n = 45$), Tanzania ($n = 13$), Thailand ($n = 15$), United Kingdom ($n = 47$), the United States ($n = 16$), and elsewhere ($n = 24$). Over half of the sera ($n = 117$ [57.1%]) were selected randomly, and the remaining 88 sera were prescreened against 6 to 12 viruses to identify and exclude weakly neutralizing sera from larger banks of sera.

A heat map summarizing 44,758 pAUC neutralization values is



shown in Fig. 1. This heat map showed that the viruses did not segregate into a practical number of clear neutralization patterns. If they had, it might have been possible to define HIV-1 neutralization serotypes, which was one of the goals of the overall study that would have provided a rationale for reference strain selection. In the absence of defined neutralization serotypes, the AUC-MB of each serum sample was used as a measure to describe the spectrum of neutralizing activity seen among all serum samples. AUC-MB was determined using individual pAUC values for a given serum sample across a set of viruses, where the pAUC values were highly correlated with ID₅₀ values of >20 (Pearson's $r = 0.91$) and provided greater sensitivity (i.e., quantifiable values when the ID₅₀ was <20) (Fig. 2A) for robust statistical analysis. For each serum sample, quartiles (i.e., 25th, 50th, and 75th percentiles) were used to sort the viruses into four equal-size groups. The least sensitive 25% of viruses have a pAUC value below the 1st quartile, and the most sensitive 25% of viruses have a pAUC value above the 3rd quartile. The 2nd quartile is the median pAUC for a serum sample. These quartiles were used as a basis to identify subsets of isolates that accurately predicted the observed MB curves. The area between curves (ABC) of the predicted and observed MB curves, where the predicted curve was based on a proposed set of reference viruses and the observed curve was based on the full set of viruses, was used to judge the accuracy of the predicted curve, where smaller values reflect greater accuracy.

A subpanel of viruses was sought that most accurately predicted the observed MB curves by using 205 sera and 195 of 219 Env-pseudotyped viruses without missing observations. We compared the abilities of K isolate panels (with K ranging between 1 and 20) to predict the AUC-MB of each serum across 195 isolates using the AUC-MB lasso model selection method with a null distribution obtained by random selection. From this analysis, a panel size of nine viruses seemed a reasonable trade-off among prediction accuracy and diminishing returns of prediction accuracy with larger panels (Fig. 2B), where the predictive value of an optimal panel of nine viruses (see below) had an R^2 value of 0.94. A panel size of nine viruses also minimizes the resources required for high-throughput testing of the large numbers of samples anticipated in vaccine trials and allowed for the addition of three strains selected based on other criteria beyond the ABC that may be relevant to future vaccine trials.

Optimal isolates that should comprise the nine-virus panel were determined using quartile prediction methods, as illustrated in Fig. 3 for serum 100008. Because pAUC values in MB curves were sorted to compute quartiles from the cumulative distribution, the particular ordering of isolates was specific to each serum

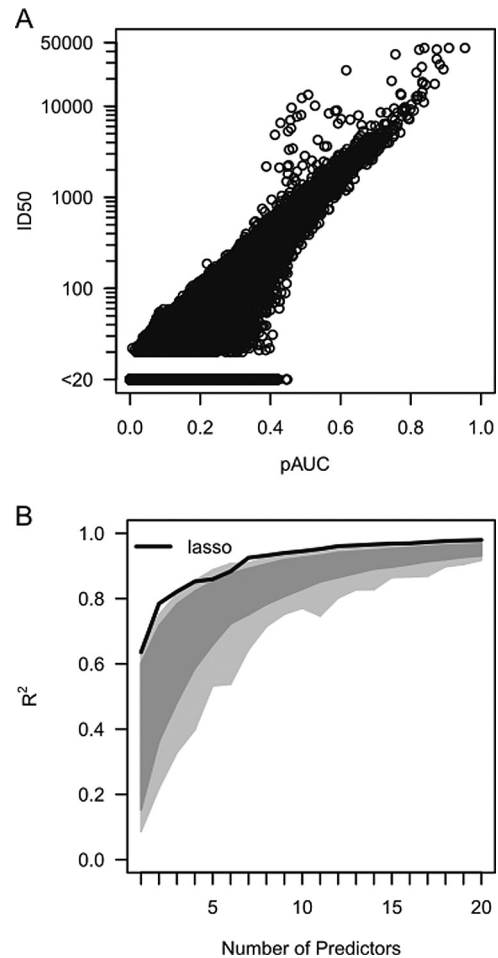


FIG 2 Use of pAUC for comparisons among optimized and randomly selected virus panels. (A) Comparison of pAUC and ID₅₀ values for all 44,758 neutralization results shown in Fig. 1. (B) R^2 values for predicting AUC-MB are shown for each of the K predictors per panel. The solid line corresponds to the optimized K isolate panels, with K ranging between 1 and 20, selected using the AUC-MB lasso panel selection method described in Materials and Methods. The dark gray region shows the range of R^2 values from the middle 95% of random panels. The light gray region shows the full distribution of R^2 values across 1,000 random panels.

and did not necessarily follow Fig. 3. Table 1 summarizes isolates in panels chosen by quartile methods, together with subtype and infection stage. Four viruses were identified by all three quartile methods, and four more were identified by Q₂ and either Q₁ or Q₃.

FIG 1 Heat map of 44,758 neutralization results from 205 chronic assayed sera against 219 Env-pseudotyped virus isolates. Positive area under the curve (pAUC) values summarize areas integrated under the dilution curve of each neutralization assay. A color key histogram in the upper left corner summarizes ranges of pAUC values depicted by heat map colors. Low pAUC values (white and lighter-colored cells) indicate no detectable neutralization and relatively weak neutralization, respectively. High pAUC values (orange and red cells) indicate moderate and potent neutralization, respectively. Gray cells indicate 137 missing observations. Colored bands above and to the left of the heat map indicate the subtypes of each serum and virus, respectively. For 34 sera, subtype information was unknown because genome amplification was unsuccessful (NA) (gray bars). Subtypes designated "Other" are noncirculating recombinant forms and two scantily represented CRFs. Leaves on dendrograms are colored to indicate the selection method by which viruses were chosen for the global reference panel (left) and which sera were selected randomly versus those that were prescreened (top). Red dots on dendrograms indicate nodes with at least 60% bootstrap support from 1,000 resampled replicates. Neutralization profiles of isolates selected by quartile-based methods and the additional reference strains are duplicated below the heat map to highlight their neutralization susceptibility. The nine strains selected for the global reference panel using the quartile Q₂ (median) are indicated in magenta. The three augmenting strains selected to complete the global reference panel are in blue. Additional strains identified using quartiles Q₃ (25th percentile) and Q₁ (75th percentile) that were not included in the global reference panel are shown in gray. Names of virus isolates, prefixed by subtype, are (from top to bottom) as follows: Q₂, C|ICE0217, 01|CNE55, B|TRO11, G|X1632, A|C|246F3, 07|CH119, C|CE1176, 07|BJOX2000, and C|25710; Q₁, C|3728, B|RPW-0510.2, 07|CH111.8, and 01|C1080.C03; Q₃, C|7060101641A7(REV-) and C|DU123.6; and the augmenting strains, B|X2278, 01|CNE8, and A|398F1.

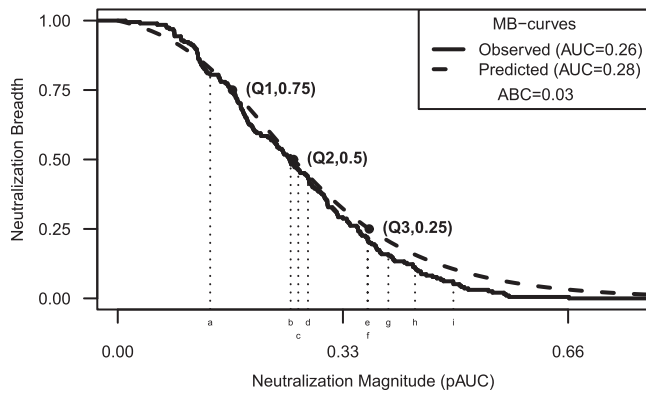


FIG 3 An example of predicting the magnitude-breadth curve for one serum. Results are shown for serum 100008 from a chronic HIV-1 subtype C-infected individual who was among the more potent neutralizers. Values along the *x* axis indicate the magnitude of neutralization potency as positive area under the titration curve (pAUC) values. Values along the *y* axis indicate neutralization breadth as the cumulative proportion of isolates having neutralization potency (pAUC) no less than the magnitude on the *x* axis. The prediction target is the magnitude-breadth (MB) curve across 195 viruses assayed with this serum (solid line). Quartiles of the distribution for this serum (Q_1 , Q_2 , and Q_3) are predicted from 9-isolate panel pAUCs given by Q_2 . Viruses a to i represent CE0217, CE1176, CH119, CNE55, 25710, TRO11, X1632, BJOX2000, and 246F3, respectively. The predicted MB curve is the logistic function fit to quartile estimates (dashed line). The inset includes the AUC-MB for both the observed and predicted MB curves along with the area between the two curves (ABC).

The Q_2 method and a multivariate predictor using all three quartiles (not shown) selected the same nine isolates. Figure 4 shows panel-based predicted MB curves from the nine-isolate Q_2 panel as assessed by ABC for the best percentile, the 33rd and 66th percentiles, and the worst fits.

Figure 5 shows the ABC goodness of fit of each predicted MB curve versus the AUC-MB and that ABC increases with serum potency. All selection methods predicted MB curves at or below an ABC threshold of 0.05 for 95.6% of sera. That is, 196 of 205 sera were fit with less than 5% ABC, leaving 9 sera as poorly fit outliers. These sera represented a variety of AUC-MB values. Figure 6 and Table 2 compare the ABC values from quartile-based selection methods obtained using the entire neutralization data set and by cross-validation. Although distributions predicted by cross-validation did not fit as well as those predicted using the entire data set, we saw minimal performance degradation when predicting independent sera.

After choosing a nine-isolate Q_2 panel of Env-pseudotyped viruses as highly predictive of neutralization profiles of 205 diverse sera from chronic infections, we noted a disproportionate number of the viruses belonged to clade C in whole or in part: three pure C clade viruses, two CRF07s (a circulating recombinant lineage common in China that is essentially C clade in Env), and one recombinant AC virus together constitute two-thirds of the selected Q_2 panel (Fig. 1 and Table 1). Only one B clade isolate, dominant in the United States and Europe, one CRF01 isolate, dominant in Thailand and parts of Asia, and one G clade isolate were included in the Q_2 panel of nine viruses. Moreover, these nine isolates spanned a limited number of neutralization clusters (Fig. 1). We therefore augmented the nine-virus panel by adding three viruses, one each from clades A, B, and CRF01, that may have the potential to detect clade-specific bnAb responses in regions of the world where some vaccine trials are being planned, outside southern Africa, where C clade dominates the epidemic. To improve sensitivity for low-level serological activity, we specifically selected the three augmenting viruses to be among those with higher susceptibility in the lower-level serological reactivity range: i.e., we selected them specifically to represent clusters in the

TABLE 1 Isolates chosen by lasso (constrained regression) quartile-based selection methods

Isolate original name	Isolate common name	Accession no.	Quartile			Clade	Stage ^d
			Q_1	Q_2	Q_3		
246_F3_C10_2 ^b	246F3	HM215279	X	X	X	AC	I
CE1176_A3 ^b	CE1176	FJ444437	X	X	X	C	E
CNE55 ^b	CNE55	HM215418	X	X	X	CRF01	L
X1632_S2_B10 ^b	X1632	FJ817370	X	X	X	G	L
CE703010217_B6 ^b	CE0217	FJ443575	X	X		C	I
BJOX002000.03.2 ^b	BJOX2000	HM215364		X	X	CRF07	E
HIV_25710-2.43 ^b	25710	EF117271		X	X	C	I
TRO.11 ^b	TRO11	AY835445		X	X	B	E
CH119.10 ^b	CH119	EF117261		X		CRF07	L
3728.v2.c6		HM215307	X			C	E
C1080.c03		JN944660	X			CRF01	L
CH111.8		EF117258	X			CRF07	L
RPW-0510.2		HM215435	X			B	U
7060101641A7(REV-)		FJ444059			X	C	E
DU123.6		DQ411850			X	C	I
X2278_C2_B6 ^c	X2278	FJ817366	NA ^d		NA	B	I
CNE8 ^c	CNE8	HM215427	NA		NA	CRF01	L
398_F1_F6_20 ^c	398F1	HM215312	NA		NA	A	NK

^a Infection stage of sample from which virus was isolated, where known: E (early), Fiebig stages I to IV; I (intermediate), Fiebig stages V and VI; L (late), Fiebig stage VI to chronic. NK, not known.

^b Nine isolates were selected for the global panel.

^c Three isolates were used to augment the global panel by representing additional neutralization clusters and genetic diversity.

^d NA, not applicable.

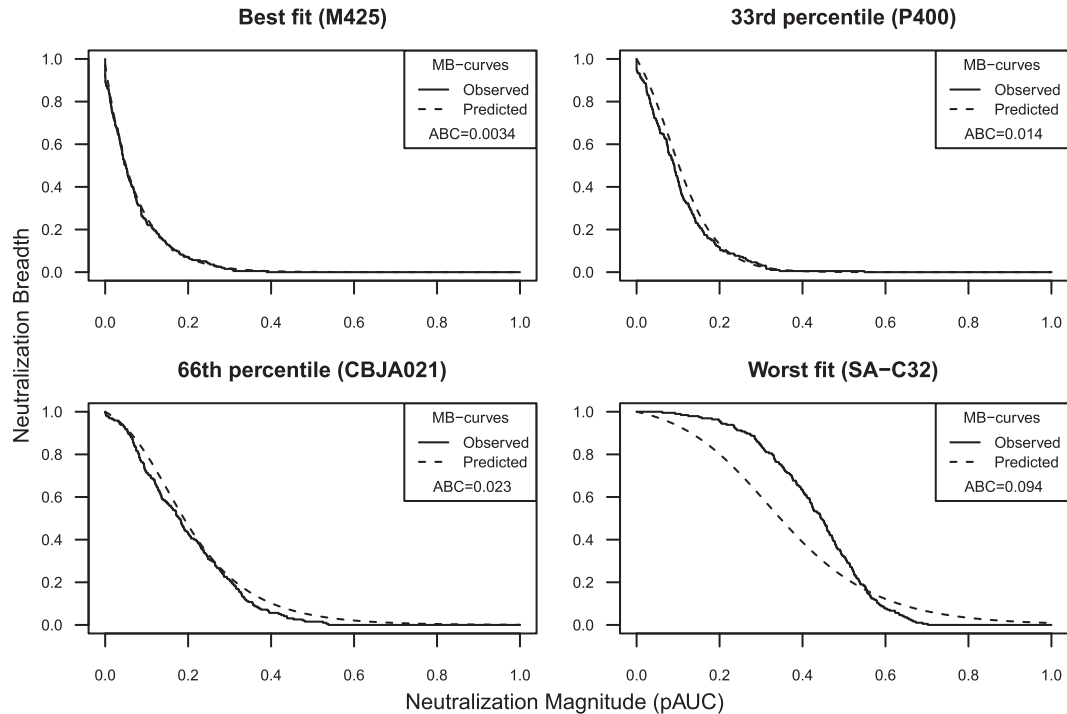


FIG 4 Magnitude-breadth curves show varied prediction outcomes. Curves are shown for the best, 33rd percentile, 66th percentile, and worst-fit sera, based on ABC from the 9-isolate Q_2 panel. The observed MB curves are shown as solid lines. The predicted MB curves appear as dashed lines. Insets report the area between the observed and predicted MB curves (ABC). Serum designations are shown in parentheses above each plot.

bottom of the plot shown in Fig. 1, which are more sensitive to the weaker sera on the left side of the heat map. Thus, these three viruses represent clusters of serum neutralization profiles not otherwise included, for a total of 12 virus isolates (Fig. 1 and Table 1), and combined they capture some reactivity missed by the Q_2 panel of nine viruses and enrich for major epidemic HIV-1 clades. These 12 isolates are listed by their original names and by abbreviated common names; the latter names are used hereafter.

Comparisons to subtype-specific panels. To gain a better understanding of the overall predictive value of the global panel, we compared its performance to that of panels comprised exclusively of either B, C, or non-B/non-C subtype viruses. Only minor pen-

alties were seen when the nine-virus global panel was used in place of a subtype-matched panel (Table 3). Here, both B and C clade subsets slightly outperform the global panel, regardless of method used. Q_2 best predicted global MB curves (i.e., target = global, panel = global, and method = Q_2), while Q_3 slightly outperformed Q_2 on subtype-specific MB curves (e.g., target = B clade, panel = global, method = Q_3 versus Q_2). When comparing the 12-isolate augmented global Q_2 panel with the 9-isolate panel,

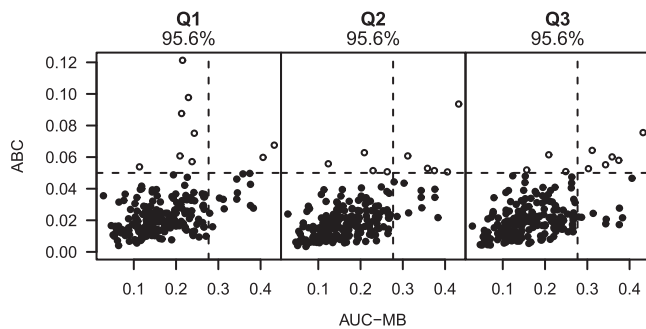


FIG 5 The area between curves quantifies the goodness of fit of predicted magnitude-breadth curves for nine-isolate panels. For each selection method, ABC versus the AUC-MB is plotted. A cutoff of ABC equal to 0.05 is indicated with a dashed horizontal line. The top 7% of neutralizers fall to the right of the dashed vertical line. Points that fall above the threshold are open, and those below the threshold are solid. The percentage of sera below the threshold criterion is given above each panel (all are 95.6%).

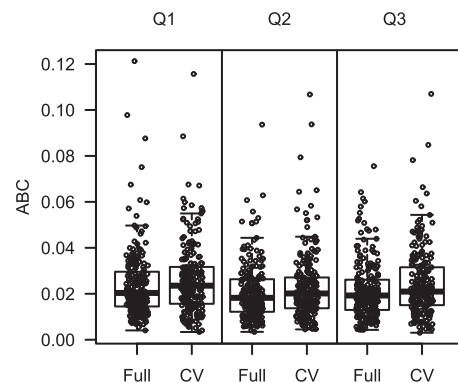


FIG 6 Ten-fold cross-validation of panel selection. The ABC goodness of fit values are compared across the three panel selection methods based on nine-isolate panels. ABC values for each serum sample are plotted using the full data set (left side of each panel) and for 10-fold cross-validation (CV) data sets (right side of each panel). Box plots are superimposed on the distribution. The midline of the box denotes the median, and the ends of the box denote the 25th and 75th percentiles. The whiskers that extend from the top and bottom of the box extend to the most extreme data points that are no more than 1.5 times the interquartile range.

TABLE 2 Panel selection 10-fold cross validation results

Panel	ABC ^a			
	Mean	SD	Median	MAD
Q ₁				
Full	0.0241	0.0154	0.0204	0.0103
CV ^b	0.0264	0.0155	0.0235	0.0119
Q ₂				
Full	0.0208	0.0125	0.0182	0.0111
CV	0.0228	0.0146	0.0201	0.0102
Q ₃				
Full	0.0216	0.0125	0.0192	0.0096
CV	0.0245	0.0150	0.0210	0.0114

^a ABC, area between curves; SD, standard deviation; MAD, median absolute deviation.

^b CV, 10-fold cross-validation.

the differences were quite minor (Table 4). When comparing the 12-isolate augmented Q₂ panel with previously defined panels for subtypes B and C (35, 36), the global panel performed best across all subtype-specific targets (Table 4).

Influence of serum potency. We evaluated the influence of highly potent sera on quartile-based serum panels as fitted versus residual values from predicted neutralization scores (Q₁, Q₂, or Q₃ in Fig. 7). For Q₁, the top three residuals in absolute value across all

TABLE 3 Goodness-of-fit comparisons between subtype-specific and global nine-isolate panels

Target	Panel	Method	Mean ABC ^a	R ² for AUC-MB ^b
Global	Global	Q ₁	0.0241	0.9116
		Q ₂	0.0208	0.9414
		Q ₃	0.0216	0.9345
B clade	Global	Q ₁	0.0317	0.8226
		Q ₂	0.027	0.9026
		Q ₃	0.0265	0.9077
	B clade	Q ₁	0.0229	0.9426
		Q ₂	0.022	0.9483
		Q ₃	0.0219	0.9495
C clade	Global	Q ₁	0.0378	0.8032
		Q ₂	0.0349	0.8814
		Q ₃	0.0339	0.8884
	C clade	Q ₁	0.0331	0.8959
		Q ₂	0.0317	0.9133
		Q ₃	0.0298	0.9298
Non-B/non-C	Global	Q ₁	0.029	0.8671
		Q ₂	0.0256	0.8959
		Q ₃	0.026	0.8876
	Non-B/non-C	Q ₁	0.0237	0.9239
		Q ₂	0.0226	0.9383
		Q ₃	0.0232	0.936

^a ABC, area between curves.

^b AUC-MB, area under the magnitude-breadth curve.

TABLE 4 Performance of global and subtype-specific panels^a

Target	Panel ^b	Mean ABC ^c	R ² for AUC-MB ^d
Global	Global _A	0.0194	0.952
	Global ₉	0.0198	0.949
	B clade	0.0338	0.744
	C clade	0.0295	0.827
B clade	Global _A	0.0201	0.932
	Global ₉	0.021	0.927
	B clade	0.0252	0.862
	C clade	0.0309	0.738
C clade	Global _A	0.0258	0.934
	Global ₉	0.0266	0.929
	B clade	0.0326	0.889
	C clade	0.0327	0.862
Non-B/non-C	Global _A	0.0211	0.928
	Global ₉	0.0217	0.928
	B clade	0.0316	0.755
	C clade	0.0293	0.796

^a Results in boldface represent the augmented Q₂ 12-isolate global panel (Global_A).

^b Global₉, Q₂ 9-isolate global panel. The 12-isolate clade B and C panels were defined previously.

^c ABC, area between curves.

^d AUC-MB, area under the magnitude-breadth curve.

sera were among the most potent. For Q₃, residuals of top neutralizers were generally positive (underpredicted), while for Q₂, residuals of top neutralizers were consistent with all sera. Top neutralizers had the highest ABC but were not atypical as outliers (Fig. 5). The Q₂ panel best predicted MB curves and performed well in cross-validation and predicted subtype-specific MB curves almost as well as Q₃. Highly potent sera did not dominate Q₂.

Choosing the optimal panel selection method. We chose Q₂ for the overall nine-isolate panel based on four factors: (i) performance based on ABC goodness of fit, (ii) cross-validation, (iii) comparison to subtype-specific panels, and (iv) influence of serum potency. Based on our analyses of these four performance criteria, Q₂ consistently performed best or with similar characteristics to the other two selection criteria.

Sequence analysis of the global reference Env panel. Analysis of full-length gp160 sequences from the 12-virus global panel showed them to be genetically diverse among a wide spectrum of heterologous strains (Fig. 8) and among each other (Fig. 9). The greatest amino acid sequence diversity was seen in the canonical

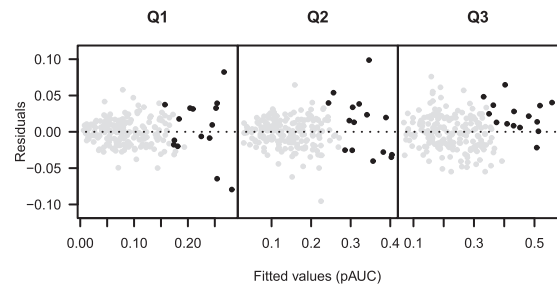


FIG 7 Influence of highly potent sera on regression. Residual and fitted pAUC values from unconstrained linear regression are depicted for each panel selection method. Highly potent sera appear as solid black circles.

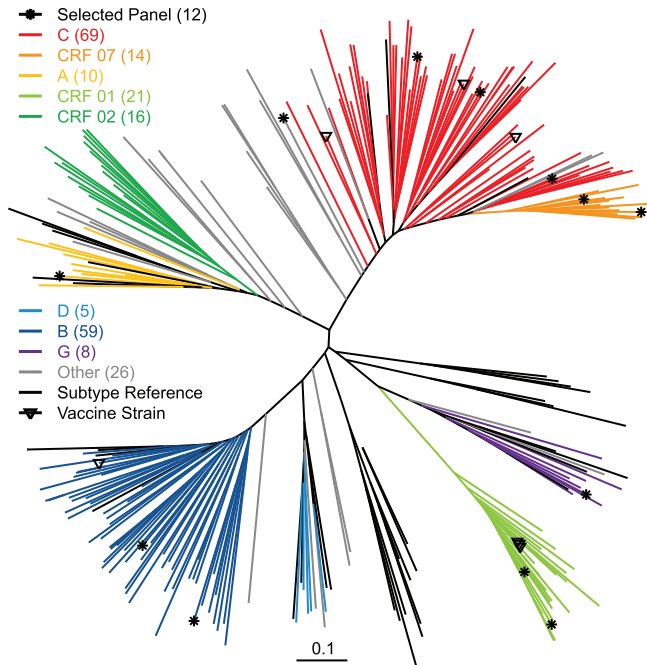


FIG 8 Phylogenetic distribution of Env-pseudotyped viruses with the selected panel shown. Branch colors indicate HIV-1 Env subtypes. This maximum likelihood tree was inferred with PhyML with the HIVb substitution model. It depicts HIV-1 group M diversity and the diverse distribution of virus isolates considered for inclusion in the global panel.

V1, V2, V3, V4, and V5 regions and in a region of approximately 32 amino acids in the N-terminal half of C3 in gp120 that included the α -2 helix (Fig. 9). The V1, V2, and V4 cysteine-cysteine (Cys-Cys) loops also exhibited substantial length variation (Table 5), whereas the V3 Cys-Cys loop did not vary in length (33 amino acids in all clones). The gp120s contained an average of 25 (range, 22 to 29) potential N-linked glycans (PNLG) (Table 5), 8 of which were 100% conserved among all 12 clones, including positions 156, 160, 276, and 301 (HXB2 numbering), which are required for known glycan-dependent bnAbs (48, 78–80) (Fig. 9). Glycans at positions 234 and 332, which are also required for certain bnAbs (48, 78), were present in 11 and 8 strains, respectively. The number ($n = 4$) and position of PNLG in the gp41 ectodomain were highly conserved (Table 5 and Fig. 9). Positions associated with neutralization by VRC01 and VRC01-like bnAbs were, for the most part, highly conserved and contained neutralization-sensitive residues (81, 82). Nine of these sites were 100% conserved (N280, R304, I420, I423, Y435, R456, G458, G459, and G471; HXB2 numbering). Minor variation of 1 or 2 amino acids occurred at the remaining six positions.

Coreceptor tropism and neutralization properties of the global panel as Env-pseudotyped viruses. It was important to determine whether the 12 viruses in the global panel were R5 tropic and possess a tier 2 neutralization phenotype that is typical of most circulating strains. All 12 Env-pseudotyped viruses were highly sensitive to the R5 inhibitor TAK-779 (50% inhibitory concentrations [IC_{50}], <0.003 to 0.68 μ M) and were relatively resistant to the X4 inhibitor AMD 3100 (IC_{50} , >5 μ M), indicating that they are R5 tropic. Figure 10 shows the neutralization sensitivity of all 219 Env-pseudotyped viruses assayed in TZM-bl cells with HIV-1 serum samples. With one exception, all viruses were sub-

stantially less sensitive than the prototypic tier 1A and tier 1B viruses, SF162.LS and Bx08, respectively, and therefore may be considered tier 2, although a small subset of the least sensitive viruses might be classified as tier 3. All global panel viruses possessed a tier 2 neutralization phenotype as Env-pseudotyped viruses, including several that were among the more sensitive viruses within this tier (Fig. 10).

In addition to being genetically diverse and exhibiting a tier 2 neutralization phenotype in TZM-bl cells, it was important to determine how well the global panel detected known bnAbs. As shown in Table 6, all 12 global panel viruses were sensitive to multiple bnAb specificities. Most viruses were sensitive to the CD4bs bnAbs VRC01 and VRC-CH31, the V1V2 glycan-dependent bnAbs PG9, PG16, and CH01, the V3-V4/glycan-dependent bnAb PT128, and the gp41 MPER-specific bnAb 4E10. Among the CD4bs bnAbs, only one virus (BJOX2000) was resistant to VRC01 and VRC-CH31; this resistance was not associated with known resistance mutations. The same virus was resistant to two additional CD4bs bnAbs, HJ16 and IgG1b12. Overall, six viruses were sensitive to HJ16, and only one was sensitive to IgG1b12. Relative bnAb breadth against the 12-virus panel mostly agrees with findings from a much larger virus panel (83). Notably, inclusion of the three strains to augment the Q_2 set of nine viruses enabled an improved capacity to detect moderately cross-reactive bnAbs, such as IgG1b12 and 2G12.

Among the glycan-dependent bnAbs, all viruses except 398F1 were sensitive to PG9 and PG16. This single resistant virus possessed N-linked glycans at positions 156 and 160 that are often required for the PG9/PG16 epitope (46, 80), suggesting that resistance was related to amino acid contacts. Ten viruses were highly sensitive to PGT128. One PGT128-resistant virus, CNE55, lacked an N-linked glycan at position 332 that is often required for the epitope (48). A second resistant virus, X1632, shifted the glycan downstream by two residues. Notably, two additional viruses, CNE8 and 246F3, showed an identical shift in the glycan but remained highly sensitive to PGT128. Overall, this panel of viruses represents multiple variations of the PGT128 epitope. Only three viruses were sensitive to 2G12. Most 2G12-resistant viruses contained subtype C sequences and lacked an N-linked glycan at position 295 that is required for the epitope and is often absent in subtype C (36).

Between the two gp41 MPER-specific bnAbs tested, 4E10 neutralized all 12 panel viruses, whereas 2F5 neutralized six. The six 2F5-sensitive viruses contained a DKW motif that has been shown to be minimum requirement for neutralization (35, 50, 84). Five 2F5-resistant viruses contained a DSW motif, while a sixth resistant virus contained a DNW motif (Fig. 9).

Coreceptor tropism and neutralization properties of the global panel as Env.IMC.LucR viruses. The 12 global reference Env clones were converted to Env.IMC.LucR viruses for greater assay utility. As one example, A3R5 cells express much lower levels of CD4 and CCR5 than TZM-bl cells and are substantially more sensitive for detecting neutralization (69, 71), especially with vaccine-elicited antibodies (85). Replication-competent Env.IMC.LucR viruses expressing *env* genes of choice in *cis* are required for this assay because most Env-pseudotyped viruses do not generate adequate RLU for accurate measurements of neutralization (67).

The viruses retained their R5 tropism as Env.IMC.LucR viruses

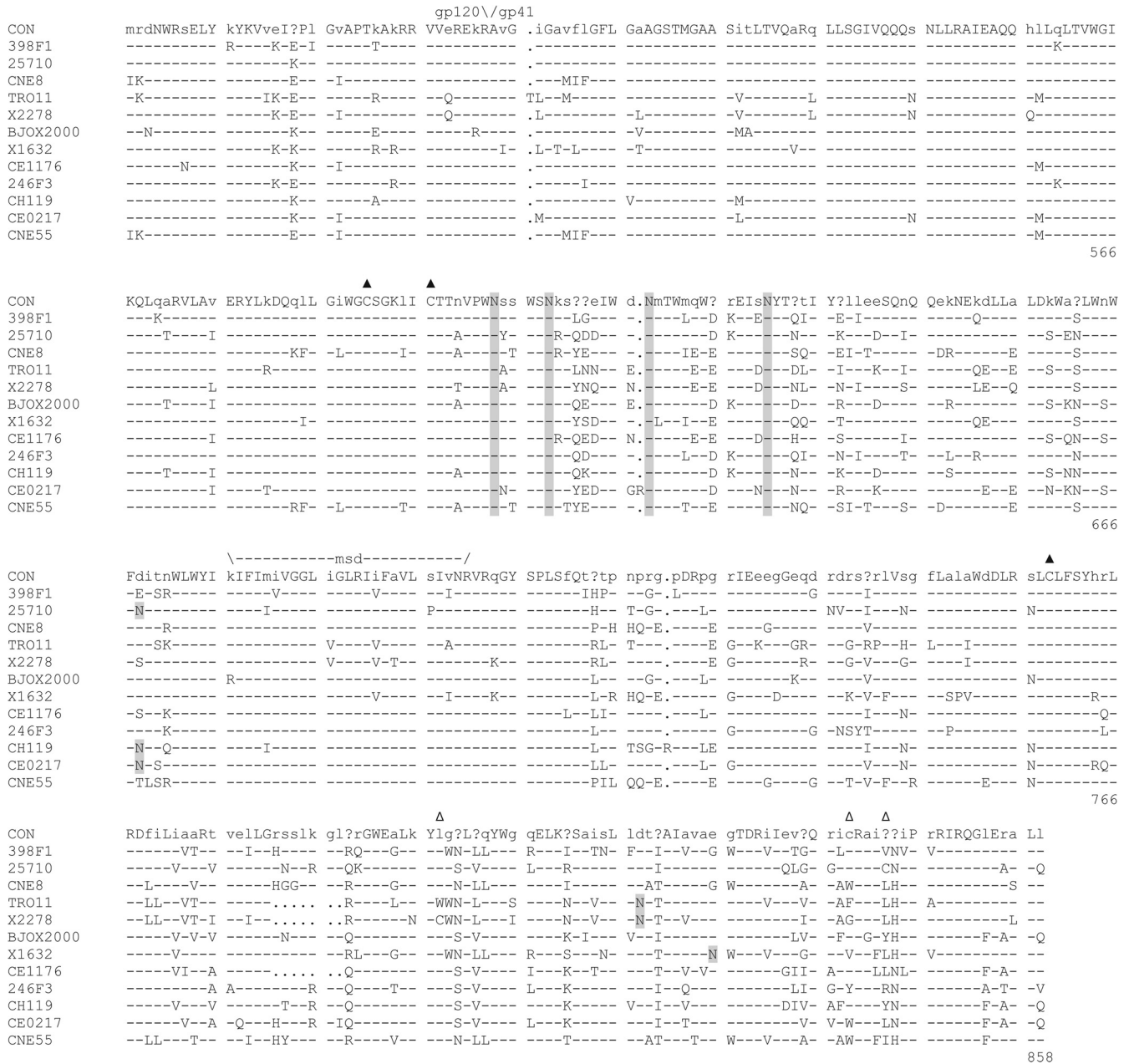


FIG 9 Alignment of deduced amino acid sequences from the 12-isolate global panel of reference Env clones. Nucleotide sequences were translated, aligned, and compared with a consensus of the 12 sequences using Clustal, where the consensus sequence was created with Consensus Maker. Numbering of amino acid residues begins with the first residue of gp120 and does not include the signal peptide. Dashes denote sequence identity, while dots represent gaps introduced to optimize alignments. Capital letters in the consensus sequence indicate 100% sequence conservation. Small letters indicate sites at which fewer than 100% but >50% of the viruses share the same amino acid residue. “?” indicates sites at which fewer than 50% of viruses share a amino acid residue. Triangles above the consensus sequence denote cysteine residues. (Solid triangles indicate sequence identity, while open triangles indicate sequence variation.) V1, V2, V3, V4, and V5 regions designate hypervariable HIV-1 gp120 domains, as previously described. The signal peptide and Env precursor cleavage sites are indicated; “msd” denotes the membrane-spanning domain in gp41. Potential N-linked glycosylation sites (NXYX motif, where X is any amino acid other than proline and Y is either serine or threonine) are shaded gray. Positions of N-linked glycans that are part of broadly neutralizing epitopes are indicated: N156 and N160 (e.g., PG9), N234 and N276 (e.g., 8ANC195 and HJ16), and N301 and N332 (e.g., PGT128). Also shown is the position of a lysine (K) residue in V2 that was a site of immune pressure in RV144. Asterisks are used to show sites that are associated with resistance to broadly neutralizing CD4bs antibodies (HXB2 positions 121, 179, 202, 279, 280, 304, 420, 423, 424, 435, 456, 458, 459, 471, and 474).

assayed in A3R5 cells, as determined by high sensitivity to TAK-779 (IC₅₀, <0.003 to 0.36 μM) and relative insensitivity to AMD 3100 (IC₅₀, >5 μM). Their tier neutralization phenotypes were examined in both A3R5 and TZM-bl cells using a multisubtype

panel of 14 serum samples from HIV-1 chronically infected individuals (subtypes A, B, and C). For comparison, two prototypic tier 1 Env.IMC.LucR viruses (MW965 and SF162) were assayed with the same samples. In agreement with the known increased

TABLE 5 Lengths of Cys-Cys variable loops and number of PNLG in the Env global panel

Isolate	No. of residues in gp120 Cys-Cys loop ^a :				No. of PNLG ^b in ^a :	
	V1 (132–156)	V2 (158–195)	V3 (297–330)	V4 (386–417)	gp120 (1–511)	gp41 ectodomain (512–684)
398F1	19	39	33	29	23	4
25710	14	43	33	31	25	5
CNE8	24	37	33	26	25	4
TRO11	30	42	33	28	29	4
X2278	27	38	33	29	27	4
BFOX2000	20	39	33	28	24	4
X1632	25	41	33	26	22	4
CE1176	21	38	33	30	27	4
246F3	20	42	33	26	25	4
CH119	19	44	33	30	25	5
CE0217	15	46	33	24	24	5
CNE55	23	40	33	18	24	4
Mean	21.4	40.8	33	27.1	25	4.3

^a In parentheses are shown the positions by the standard HXB2 numbering of each Env clone region as defined in the Los Alamos HIV database (<http://www.hiv.lanl.gov/content/sequence/HIV/MAP/annotation.html>).

^b PNLG, potential N-linked glycans.

sensitivity of the A3R5 assay, all members of the global panel of Env.IMC.LucR viruses were substantially more sensitive to neutralization in A3R5 than in TZM-bl cells (Fig. 11). The sensitivity of the three Env.IMC.LucR viruses used to augment the global panel (398F1, CNE8, and X2278) overlapped that of the prototypic tier 1 viruses MW965.IMC.LucR and SF162.IMC.LucR in A3R5 cells, and therefore these viruses are considered to possess a tier 1 neutralization phenotype in this assay. Notably, CNE8.Env.IMC.LucR and X2278.Env.IMC.LucR exhibited a tier 2 phenotype in TZM-bl cells, as did the corresponding Env-pseudotyped viruses (Fig. 10). We have seen multiple cases of Env.IMC.LucR viruses exhibiting a phenotype switch in the two cell types; these viruses tend to be at the more sensitive end of the tier 2 spectrum in the TZM-bl assay (unpublished data). The three augmentation viruses were selected for being among the most susceptible to weakly neutralizing sera in the TZM-bl assay, which may explain in part why they were the only members of the 12 virus global panel to exhibit a tier 1 phenotype in A3R5 cells. The remaining nine global panel Env.IMC.LucR viruses exhibited a spectrum of tier 2 neutralization phenotypes in A3R5 cells.

An unexpected finding was one virus, 398F1, which exhibited a tier 1 phenotype as an Env.IMC.LucR virus in both cell types but was tier 2 when assayed as an Env-pseudotyped virus in TZM-bl cells. This is the first example we have seen of such a wide discrepancy between the two different molecular Env constructs assayed in TZM-bl cells. The two constructs differ in the cytoplasmic tail (CT) of gp41, which is derived from NL4-3 in the case of the Env.IMC.LucR viruses used here. Thus, the Env.IMC.LucR viruses contained only the ectodomain (ecto) of the designated strain, whereas the Env-pseudotyped viruses contain full-length gp160. We examined whether gp41CT might affect the neutralization phenotype of this virus by assaying an Env.IMC.LucR.RE virus containing the entire *rev-env* region (i.e., full-length gp160) of HIV-1 strain 398F1. The latter Env.IMC.LucR.RE virus was substantially less sensitive to neutralization by the 14 HIV-1 sera than the corresponding ecto version of the Env.IMC.LucR virus in TZM-bl cells (geometric mean titers [GMT] of 108 and 17,160,

respectively), where the Env.IMC.LucR.RE more closely resembled the neutralization susceptibility of the Env-pseudotyped virus assayed in TZM-bl cells with the same 14 HIV-1 sera (GMT of 105). Both forms of the Env.IMC.LucR viruses exhibited a highly sensitive tier 1 phenotype with the 14 HIV-1 sera in A3R5 cells, where the RE version was slightly less sensitive to neutralization than the corresponding ecto version (GMT of 39,545 and 99,426, respectively). These results suggest that NL4-3 gp41CT dramatically altered the neutralization phenotype of this virus in TZM-bl cells, while having only a moderate effect on the phenotype in A3R5 cells.

The Env.IMC.LucR global panel viruses were further characterized with bnAbs in the A3R5 assay (Table 6). Most results were very similar to those obtained with Env-pseudotyped viruses in the TZM-bl assay. A few notable exceptions included a substantial increase in neutralization potency in the A3R5 assay when IgG1b12 was assayed with CE0217, when 2F5 was assayed with 398F1, CNE8, and X2278, and when 4E10 was assayed with 398F1, CNE8, and CE0217, all as Env.IMC.LucR viruses. Two cases of decreased potency in the A3R5 assay were noted: CH01 assayed with 398F1.IMC.LucR and 4E10 assayed with TRO11.IMC.LucR.

We sought to identify epitopes that might be responsible for the enhanced sensitivity of the A3R5 assay with HIV-1 serum samples. This was done by assaying additional MAbs that rarely neutralize tier 2 viruses in TZM-bl cells. Several of these MAbs neutralized multiple global panel viruses. The most frequently targeted epitopes were in the CD4bs, V3 loop, and CD4i regions of gp120 and in the cluster I region of gp41 (Table 7). Less frequent neutralization was seen with V2-specific MAbs, whereas neutralization by MAbs to the C2 and C5 regions of gp120 and to cluster II epitopes in gp41 was rare or absent. Overall, viruses that were more sensitive to neutralization by HIV-1 sera were more likely to be neutralized by a subset of these MAbs. One exception was 25710.IMC.LucR, which was among the most sensitive to HIV-1 sera but was resistant to all of the MAbs. Another exception was CH119.IMC.LucR, which was among the least sensitive to HIV-1 sera but was often sensitive to the V3 and CD4bs MAbs. A final exception was CNE55.IMC.LucR, which was the least sensitive to

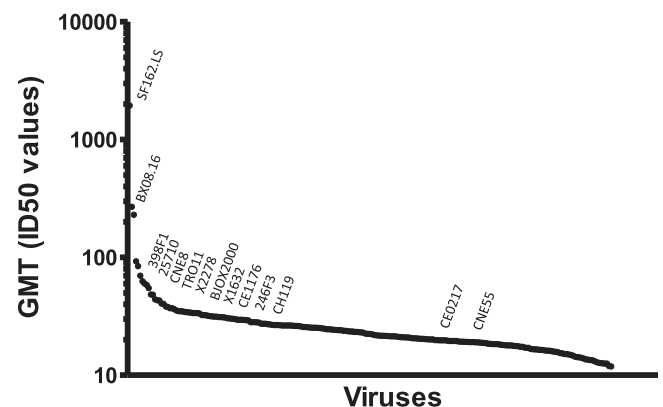


FIG 10 Neutralization phenotype of the 12-virus global panel as Env-pseudotyped viruses assayed with HIV-1 sera in TZM-bl cells. Shown are the geometric mean titers (GMT) of neutralizing activity of 205 HIV-1 sera assayed against each of 219 Env-pseudotyped viruses. For comparison, a subset of these serum samples was assayed against SF162.LS and BX08.16 as prototypic tier 1A and tier 1B viruses, respectively. The approximate location of each global panel Env-pseudotyped virus is indicated.

TABLE 6 Highly conserved neutralization epitopes on the 12 global panel viruses as Env-pseudotyped viruses and Env.IMC.LucR viruses assayed in TZM-bl and A3R5 cells, respectively

Assay	MAb	IC ₅₀ (μg/ml) ^a											
		398F1 ^b	25710	CNE8 ^b	TRO11	X2278 ^b	BJOX2000	X1632	CE1176	246F3	CH119	CE0217	CNE55
TZM-bl	VRC01	0.20	1.4	0.80	0.43	0.14	>25	0.12	2.25	0.30	1.20	0.30	0.30
A3R5		0.24	0.69	0.37	0.33	0.07	>25	0.09	1.95	0.39	0.68	0.32	0.13
TZM-bl	VRC-CH31	0.06	0.40	0.08	0.12	0.11	>25	0.01	1.49	0.03	1.8	0.05	0.04
A3R5		0.19	0.27	0.09	0.07	0.04	22	0.03	0.57	0.07	1.1	0.05	0.03
TZM-bl	HJ16	>25	>25	24	0.08	>25	>25	>25	0.14	24	0.14	0.05	>25
A3R5		>25	>25	17	0.09	>25	>25	>25	0.11	18	0.09	0.03	>25
TZM-bl	IgG1b12	0.01	>25	>25	>20	>25	>25	>25	>25	>25	>25	>25	>25
A3R5		0.05	>25	>25	>25	>25	>25	>25	>25	>25	>25	5.3	>25
TZM-bl	PG9	>5	0.07	0.60	>5	0.02	0.07	0.11	0.01	0.03	0.60	0.010	0.20
A3R5		>5	0.03	0.29	>5	0.01	0.09	0.05	0.01	0.04	0.34	0.003	0.07
TZM-bl	PG16	>5	0.01	0.50	1.92	<0.002	0.01	0.01	0.003	<0.002	0.40	<0.002	0.50
A3R5		>5	0.003	0.09	2.46	0.004	0.02	0.01	0.003	0.01	0.27	0.004	0.04
TZM-bl	CH01	0.5	1.8	>25	>25	0.08	9.1	2.1	0.04	1.3	2.4	0.28	>25
A3R5		2.8	1.9	>25	>25	0.09	>25	1.9	0.04	7.0	2.2	0.25	>25
TZM-bl	PGT128	0.01	0.07	0.02	0.02	0.02	0.05	>5	0.01	0.01	0.07	0.09	>5
A3R5		0.02	0.04	0.02	0.03	0.01	0.07	>5	0.06	0.02	0.02	0.08	>5
TZM-bl	2G12	21	>25	>25	0.40	0.20	>25	>25	>25	>25	>25	>25	>25
A3R5		>25	>25	>25	0.45	0.13	>25	>25	>25	>25	>25	>25	>25
TZM-bl	2F5	4.8	>25	1.20	>50	11.5	>25	5.5	>25	1.7	>25	>25	0.9
A3R5		0.1	>25	0.20	>25	0.7	>25	1.1	>25	2.2	>25	>25	1.4
TZM-bl	4E10	9.8	6.9	1.06	0.3	18.2	6.9	6.1	4.6	3.2	6.7	2.8	5.4
A3R5		0.1	6.5	0.07	2.6	4.0	1.6	4.1	3.0	11.9	2.2	0.2	19.8

^a Assays in TZM-bl and A3R5 cells were performed with Env-pseudotyped viruses and Env.IMC.LucR (ecto) viruses, respectively. Positive neutralization is shown in boldface.

^b Three isolates were used to augment the global panel.

HIV-1 sera but was neutralized by two gp41 cluster I MAbs. Though we did not do parallel assays in TZM-bl cells, we have assayed these same MAbs against other viruses in both A3R5 and TZM-bl cells and find that when they neutralize in A3R5 cells, the activity is rarely detected in TZM-bl cells when the same stocks of Env.IMC.LucR viruses are used in both assays (unpublished data).

DISCUSSION

We describe a practical number of Env reference strains representative of the global HIV-1 epidemic for use in performing standardized assessments of vaccine-elicited nAb responses. This new global panel was selected from among 219 tier 2 Env-pseudotyped viruses that were characterized in TZM-bl cells with 205 chronic sera from HIV-1-infected individuals. Both the Env-pseudotyped viruses and the sera were sampled globally from diverse geographic locations and together represented five HIV-1 M-group subtypes (A, B, C, D, and G), three common circulating recombinant forms (CRFs 01, 02, and 07), and additional unique recombinants. This is by far the largest and most comprehensive checkerboard-style neutralization data set reported to date for HIV-1 and therefore is best suited for reference strain selection.

A lasso statistical model selection procedure was used to analyze the neutralization data set for reference strain selection. A

global panel of reference Envs was selected based on method Q₂, which performed the best based on the ABC. Performance under cross-validation also suggests that Q₂ is the best among the quartile methods tested. The spectrum of serum neutralizing activity seen against a large multisubtype panel of 219 Env-pseudotyped viruses was shown to accurately predict results with a small subset of only nine selected viruses ($R^2 = 0.94$). This is a practical number of viruses for large-scale assessments of nAbs in preclinical and clinical stages of vaccine development.

A review of the initial selected isolates showed preference for subtype C and CRF07, the latter being a recombinant lineage that carries subtype C in Env. Of note, some of the sera used in the large checkerboard panel were selected after prescreening to exclude sera with low activity. The vast majority of prescreened sera were from individuals infected with subtype C and CRF07 viruses. In the event that intraclade sensitivity subtly impacted our selection criteria by introducing unintended bias, and because some vaccine trials are being planned in areas of the world where other subtypes predominate, three additional viruses were selected to augment the global Q₂ panel selected by lasso. Sera with similar neutralization profiles were grouped using hierarchical clustering of Euclidean distances. One subtype A virus, one subtype B virus, and one CRF01 virus were included to represent clusters of neu-

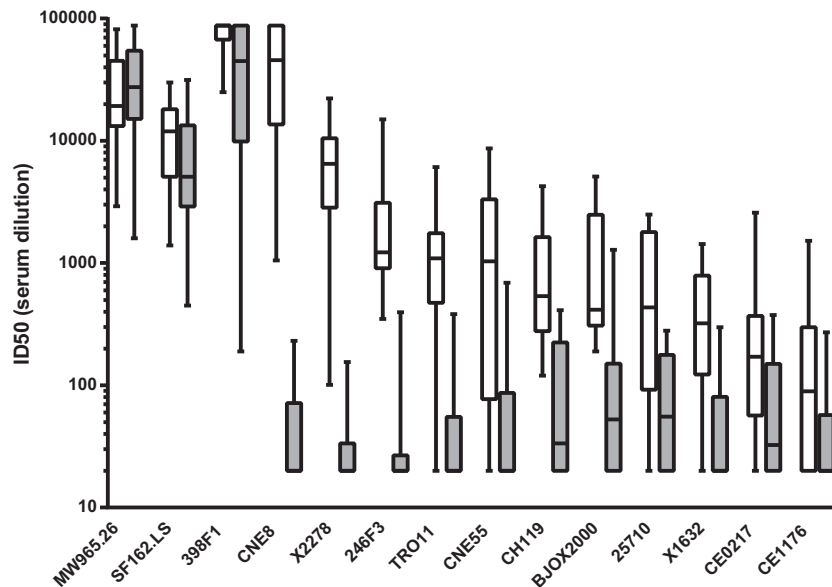


FIG 11 Neutralization phenotype of the 12 virus global panel as Env.IMC.LucR viruses assayed with HIV-1 sera in A3R5 cells and TZM-bl cells. Each Env.IMC.LucR virus was assayed in A3R5 (open boxes) and TZM-bl cells (shaded boxes) with serum samples from 14 HIV-1 chronically infected individuals (4 subtype A, 5 subtype B, and 5 subtype C). Boxes extend from the 25th to 75th percentiles of neutralization titers. Horizontal bars are the median titers.

tralization profiles not otherwise covered (Fig. 1) and to augment representation of distinct subtypes that were underrepresented in the panel of nine but that are important in terms of their high prevalence in regions where vaccine trials are likely to be conducted. The three viruses added to this panel provide additional coverage, including an improved ability to detect weaker bnAbs, while maintaining a practical panel size and predictive power.

All 12 members of the global panel were R5 tropic and exhibited a tier 2 neutralization phenotype as Env-pseudotyped viruses in TZM-bl cells. For additional utility, the global panel was shown to be nearly as good as subtype-specific panels for prediction of subtype-specific nAb responses in the TZM-bl assay. Although it is practical and reasonable to use a subtype-specific reference panel in subtype-specific settings when evaluating a vaccine for protection against limited viral diversity, as is the case when a single subtype predominates at the time and place of the trial, use of a standard set of isolates, regardless of setting, would enable comparisons across studies and provide greater opportunity to characterize immune correlates of protection against the diversity encountered in the global context of the HIV-1 pandemic. In addition, by changing the target MB curve (e.g., the observed MB curve based on the subset of subtype C viruses), these methods can adjust prediction accuracy for target virus populations of interest.

The utility of any panel of Env reference strains for HIV-1 vaccine development also depends on their ability to detect known bnAbs. In this regard, the panel selected here was highly sensitive for detecting bnAb epitopes in the CD4bs (e.g., VRC01, VRC-CH31, and HJ16), V1V2 glycan (e.g., PG9, PG16, and CH01), V3/V4 glycan (PGT128), and gp41 MPER (e.g., 2F5 and 4E10). It will be important to continue to test the sensitivity of these viruses to newer bnAbs that become available in the future.

One possible limitation of our virus panel selection method is that selection was based on responses to natural infection, whereas the primary intended use of this panel is to assess the magnitude and breadth of vaccine-elicited responses. In this regard, most of

the panel-based MB curve predictions for natural infection sera were very accurate, although a few outlier serum samples were poorly predicted. In the context of a phase I/II randomized clinical trial, summaries of sera are unlikely to be highly influenced by outlier sera, and therefore, MB curves should be predictable with sufficient accuracy to summarize neutralization profiles among the panel viruses. Moreover, by predicting distributions of neutralization values per serum (i.e., MB curve) rather than which sera will neutralize a particular virus isolate, the problem is simplified to estimating generic parameters of the neutralization distribution. Nonetheless, as vaccine trial data accrue, it may be prudent to evaluate a small subset of vaccine sera using more extensive virus panels, for direct comparison to this global panel, to determine if the predictability of the global panel based on natural infection is maintained in a vaccine context.

For greater assay utility, all 12 global panel Env clones were converted to Env.IMC.LucR viruses and shown to be suitable for nAb assays in A3R5 cells, where they retained their R5 tropism and sensitivity to known bnAbs and, as expected, were substantially more sensitive to neutralization with HIV-1 sera than were the corresponding Env-pseudotyped viruses assayed in TZM-bl cells. Their enhanced sensitivity to HIV-1 sera might be explained in part by an increased vulnerability of epitopes in the CD4bs, CD4i, and V3 regions of gp120 and cluster I epitopes in gp41 (Table 7).

Assays with these viruses in A3R5 cells should permit ultrasensitive detection of vaccine-elicited neutralizing antibodies (85). We note, however, that because the reference Envs were selected on the basis of neutralization results with Env-pseudotyped viruses in the TZM-bl assay, and because of possible qualitative differences in the neutralization specificities detected in the two assays (unpublished results), the predictive power of this panel of Env-IMC.LucR viruses assayed in A3R5 cells does not have the same level of qualification as the corresponding Env-pseudotyped viruses assayed in TZM-bl cells. For this reason, when possible, additional assays with subtype-specific and region-specific panels

TABLE 7 Additional neutralization epitopes on the 12 global panel Env.IMC.LucR viruses assayed in A3R5 cells

MAb	Epitope	IC ₅₀ (μg/ml) ^a												
		398F1 ^b	25710	CNE8 ^b	TRO11	X2278 ^b	BJOX2000	X1632	CE1176	246F3	CH119	CE0217	CNE55	
17b	CD4i	13.9	>25	10.2	>25	5.8	16.4	>25	>25	21.0	>25	>25	>25	
E51		>25	>25	>25	>25	17.5	9.8	>25	>25	>25	>25	>25	>25	
412D	V3	>18.5	>18.5	>18.5	>18.5	12.3	>18.5	>18.5	>18.5	>18.5	>18.5	>18.5	>18.5	
2219		0.71	>25	>25	>25	>25	>25	>25	>25	>25	9.6	>25	>25	
2557		0.02	>24	>24	>24	>24	15.2	11.1	>24	>24	13.3	>24	>24	
3074		0.01	>25	0.1	>25	>25	9.2	12.0	>25	>25	13.1	>25	>25	
3869		0.004	>25	>25	>25	>25	6.6	5.8	>25	>25	8.7	>25	>25	
447-52D		>25	>25	>25	12.2	8.9	>25	>25	>25	>25	>25	>25	>25	
838-D		0.06	>18	>18	>18	>18	>18	>18	>18	>18	15.9	>18	>18	
1361		V2	>25	>25	3.4	>25	>25	>25	>25	>25	>25	>25	>25	
1393A	>25		>25	2.8	>25	>25	>25	>25	>25	>25	>25	>25		
1357D (A)	>25		>25	7.5	>25	>25	>25	>25	>25	>25	>25	>25		
697-30D	17.6		>25	7.7	>25	>25	>25	>25	>25	>25	>25	>25		
830A	>25		>25	>25	>25	>25	>25	>25	>25	14.3	10.7	>25	>25	
2297	>25		>25	>25	>25	>25	>25	>25	>25	>25	>25	>25	>25	
654-30D	CD4bs		0.03	>25	>25	24.7	0.1	4.4	>25	>25	3.4	2.9	>25	>25
1008-30D			0.07	>25	>25	>25	0.3	18.6	>25	>25	13.1	4.8	>25	>25
1570D		0.04	>25	4.2	6.5	0.2	6.4	>25	>25	2.3	1.8	>25	>25	
729-30D		0.03	>25	>25	>25	0.4	4.3	>25	>25	0.6	2.5	>25	>25	
847D	C2	>25	>25	>25	>25	>25	>25	>25	>25	>25	>25	>25		
1331-160A	C5	>25	>25	>25	>25	>25	>25	>25	>25	>25	>25	>25		
670-30D		>25	>25	>25	>25	>25	>25	>25	>25	>25	>25	>25		
858-30D		1.5	>21.5	>21.5	>21.5	>21.5	>21.5	>21.5	>21.5	>21.5	>21.5	>21.5		
181D	gp41 cluster I	>25	>25	>25	3.0	0.1	>25	>25	>25	>25	>25	>25		
246D		>25	>25	1.6	3.6	0.1	>25	>25	>25	16.2	>25	15.2	>25	
240D		22.1	>25	0.06	4.4	0.7	>25	>25	>25	>25	>25	>25	>25	
50-69D		>25	>25	0.02	2.2	0.4	>25	>25	>25	24.1	>25	>25	2.0	
4B3		>25	>25	0.02	10.0	>25	>25	>25	>25	>25	>25	>25	6.7	
126-7D		gp41 cluster II	>25	>25	>25	>25	>25	>25	>25	>25	>25	>25	>25	
167D	>25		>25	>25	>25	>25	>25	>25	>25	>25	>25	>25		
1418(16)	Parvovirus b19	>25	>25	>25	>25	>25	>25	>25	>25	>25	>25	>25		
3685A	PA (anthrax)	>25	>25	>25	>25	>25	>25	>25	>25	>25	>25	>25		

^a Assays were performed with Env.IMC.LucR (ecto) viruses. Positive neutralization is shown in boldface.

^b Three isolates were used to augment the global panel.

of Env.IMC.LucR viruses should be considered for comprehensive assessments of vaccine-elicited responses in the A3R5 assay.

We note that three of the Env.IMC.LucR viruses exhibited a tier 1 neutralization phenotype in A3R5 cells, whereas all 12 reference Envs exhibited a tier 2 phenotype as Env-pseudotyped viruses in TZM-bl cells. We do not understand the basis for this phenotype “switch” from tier 2 in TZM-bl to tier 1 in A3R5 cells. It is possible that the switch is related to the use of Env-pseudotyped viruses in TZM-bl cells, which contain full-length gp160, whereas the Env.IMC.LucR viruses used in the A3R5 assay contain only the ectodomain of the virus of choice (gp41CT being derived from NL4-3). However, we have seen multiple cases of a similar phenotype switch when only Env.IMC.LucR viruses are used in both assays (unpublished data), suggesting that gp41CT is rarely responsible. Nevertheless, we did observe one special case of a

virus (398F1) in the present study that exhibited a phenotype switch possibly related to gp41CT. This virus was one of three chosen to augment the nine viruses selected by lasso. The full-length gp160 of this virus as either an Env-pseudotyped virus or Env.IMC.LucR.RE virus exhibited a tier 2 phenotype in TZM-bl cells, whereas the corresponding Env.IMC.LucR version containing the Env ectodomain of 398F1, and the gp41CT of NL4-3 exhibited a tier 1 phenotype. This is an interesting but likely exceptional case for a more detailed study of the possible influence of gp41CT on the antigenic structure of the Env ectodomain (unpublished data).

In summary, a robust statistical analysis of a large checkerboard-style neutralization data set was used to select a global panel of HIV-1 reference strains for standardized assessments of vaccine-elicited nAb responses. Unlike other panels, this one was

qualified on the basis of predicting responses to a wide range of HIV-1 variants from diverse geographic locations and was shown to predict subtype-specific responses. This represents the first panel described to date that is designed to permit standardized assessments across multiple vaccine platforms tested in different parts of the world. The large neutralization data set described here may also be used to characterize the overall probability that any serum has neutralization activity against any randomly chosen virus. We observed from the full set of neutralization assay results that this estimated probability, or population-coverage index, is unbiased (not shown). Because of this, the estimated coverage parameters could be used in power calculations for clinical trials. Estimates of population coverage might be used to predict vaccine efficacy in a clinical trial based on a sample of HIV-1 sequences circulating in the trial, data on HIV-1 exposure patterns, and a model linking the vaccine effect on the per-exposure infection probability to the neutralization potency present in a given host-virus interaction.

ACKNOWLEDGMENTS

We thank Francine McCutchan, Carolyn Williamson, Beatrice Hahn, Ronald Swanstrom, Feng Gao, Jerome Kim, Miguel Thompson, and the HIV Superinfection Study (HISIS) (Principal Investigators M. Hoelscher and L. Mabokofofor) for molecular Env clones. We also thank Lynn Morris, Guy de Bruyn, Ramesh Paranjape, Pachamuthu Balakrishnan, Yiming Shao, Kunxue Hong, Hao Wu, Ning Li, Linqi Zhang, Hong Shang, Lindsey Baden, Aine McKnight, Ruengpung Sutthent, Esper Kallas, Center For HIV/AIDS Vaccine Immunology, Centre for the AIDS Programme of Research in South Africa, International AIDS Vaccine Initiative, HIV Vaccine Trials Network, HIV Prevention Trials Network, Southern African National Blood Services, US Military HIV Research Program, Zambia-Emory HIV Research Project, and the Bill and Melinda Gates Foundation's Collaboration for AIDS Vaccine Discovery for serum specimens from HIV-1-infected subjects. We thank Dennis Burton for b12, PG9, PGT128 and PGT145, Davide Corti and Antonio Lanzavecchia for HJ16, Mark Connors for 10E8, Herman Katinger for 2G12, 2F5, and 4E10, and Barton Haynes for CH01 and CH31. We also thank the Center for HIV/AIDS Vaccine Immunology (CHAVI) and the Duke CHAVI-Immunogen Discovery (CHAVI-ID) for providing clade-classified serum samples.

This work was funded by grants from the Bill & Melinda Gates Foundation (Collaboration for AIDS Vaccine Discovery no. 38619 and 1032144) and by the Intramural Research Program of the Vaccine Research Center, NIAID, NIH. This work was further supported by the Virology Core of the Birmingham Center for AIDS Research (CFAR, AI27767).

REFERENCES

- Mascola JR, Montefiori DC. 2010. The role of antibodies in HIV vaccines. *Annu. Rev. Immunol.* 28:413–444. <http://dx.doi.org/10.1146/annurev-immunol-030409-101256>.
- Hemelaar J, Gouws E, Ghys PD, Osmanov S. 2011. Global trends in molecular epidemiology of HIV-1 during 2000–2007. *AIDS* 25:679–689. <http://dx.doi.org/10.1097/QAD.0b013e328342ff93>.
- Hemelaar J. 2013. Implications of HIV diversity for the HIV-1 pandemic. *J. Infect.* 66:391–400. <http://dx.doi.org/10.1016/j.jinf.2012.10.026>.
- Seaman MS, Janes H, Hawkins N, Grandpre LE, Devoy C, Giri A, Coffey RT, Harris L, Wood B, Daniels MG, Bhattacharya T, Lapedes A, Polonis VR, McCutchan FE, Gilbert PB, Self SG, Korber BT, Montefiori DC, Mascola JR. 2010. Tiered categorization of a diverse panel of HIV-1 Env pseudoviruses for assessments of neutralizing antibodies. *J. Virol.* 84:1439–1452. <http://dx.doi.org/10.1128/JVI.02108-09>.
- Bou-Habib DC, Roderiquez G, Oravec T, Berman PW, Lusso P, Norcross MA. 1994. Cryptic nature of envelope V3 region epitopes protects primary monocytotropic human immunodeficiency virus type 1 from antibody neutralization. *J. Virol.* 68:6006–6013.
- Davis KL, Gray ES, Moore PL, Decker JM, Salomon A, Montefiori DC, Graham BS, Keefer MC, Pinter A, Morris L, Hahn BH, Shaw GM. 2009. High titer HIV-1 V3-specific antibodies with broad reactivity but low neutralizing potency in acute infection and following vaccination. *Virology* 387:414–426. <http://dx.doi.org/10.1016/j.virol.2009.02.022>.
- Decker JM, Bibollet-Ruche F, Wei X, Wang S, Levy DN, Wang W, Delaporte E, Peeters M, Derdeyn CA, Allen S, Hunter E, Saag MS, Hoxie JA, Hahn BH, Kwong PD, Robinson JE, Shaw GM. 2005. Antigenic conservation and immunogenicity of the HIV coreceptor binding site. *J. Exp. Med.* 201:1407–1419. <http://dx.doi.org/10.1084/jem.20042510>.
- Matthews TJ. 1994. Dilemma of neutralization resistance of HIV-1 field isolates and vaccine development. *AIDS Res. Hum. Retroviruses* 10:631–632. <http://dx.doi.org/10.1089/aid.1994.10.631>.
- Moore JP, Burton DR. 2004. Urgently needed: a filter for the HIV-1 vaccine pipeline. *Nat. Med.* 10:769–771. <http://dx.doi.org/10.1038/nm0804-769>.
- Burton DR, Ahmed R, Barouch DH, Butera ST, Crotty S, Godzik A, Kaufmann DE, McElrath MJ, Nussenzweig MC, Pulendran B, Scanlan CN, Schief WR, Silvestri G, Streeck H, Walker BD, Walker LM, Ward AB, Wilson IA, Wyatt R. 2012. A blueprint for HIV vaccine discovery. *Cell Host Microbe* 12:396–407. <http://dx.doi.org/10.1016/j.chom.2012.09.008>.
- Kwong PD, Mascola JR. 2012. Human antibodies that neutralize HIV-1: identification, structures, and B cell ontogenies. *Immunity* 37:412–425. <http://dx.doi.org/10.1016/j.immuni.2012.08.012>.
- Corti D, Lanzavecchia A. 2013. Broadly neutralizing antiviral antibodies. *Annu. Rev. Immunol.* 31:705–742. <http://dx.doi.org/10.1146/annurev-immunol-032712-095916>.
- Huang J, Ofek G, Laub L, Louder MK, Doria-Rose NA, Longo NS, Imamichi H, Bailer RT, Chakrabarti B, Sharma SK, Munir Alam S, Wang T, Yang Y, Zhang B, Migueles SA, Wyatt R, Haynes BF, Kwong PD, Mascola JR, Connors M. 2012. Broad and potent neutralization of HIV-1 by a gp41-specific human antibody. *Nature* 491:406–414. <http://dx.doi.org/10.1038/nature11544>.
- Burton DR, Desrosiers RC, Doms RW, Koff WC, Kwong PD, Moore JP, Nabel GJ, Sodroski J, Wilson IA, Wyatt RT. 2004. HIV vaccine design and the neutralizing antibody problem. *Nat. Immunol.* 5:233–236. <http://dx.doi.org/10.1038/ni0304-233>.
- Douek DC, Kwong PD, Nabel GJ. 2006. The rational design of an AIDS vaccine. *Cell* 124:677–681. <http://dx.doi.org/10.1016/j.cell.2006.02.005>.
- Dey B, Svehla K, Xu L, Wycuff D, Zhou T, Voss G, Phogat A, Chakrabarti BK, Li Y, Shaw G, Kwong PD, Nabel GJ, Mascola JR, Wyatt RT. 2009. Structure-based stabilization of HIV-1 gp120 enhances humoral immune responses to the induced co-receptor binding site. *PLoS Pathog.* 5:e1000445. <http://dx.doi.org/10.1371/journal.ppat.1000445>.
- Wu L, Zhou T, Yang ZY, Svehla K, O'Dell S, Louder MK, Xu L, Mascola JR, Burton DR, Hoxie JA, Doms RW, Kwong PD, Nabel GJ. 2009. Enhanced exposure of the CD4-binding site to neutralizing antibodies by structural design of a membrane-anchored human immunodeficiency virus type 1 gp120 domain. *J. Virol.* 83:5077–5086. <http://dx.doi.org/10.1128/JVI.02600-08>.
- Ho J, Uger RA, Zwick MB, Luscher MA, Barber BH, MacDonald KS. 2005. Conformational constraints imposed on a pan-neutralizing HIV-1 antibody epitope result in increased antigenicity but not neutralizing responses. *Vaccine* 23:1559–1573. <http://dx.doi.org/10.1016/j.vaccine.2004.09.037>.
- DeVico A, Fouts T, Lewis GK, Gallo RC, Godfrey K, Charurat M, Harris I, Galmin L, Pal R. 2007. Antibodies to CD4-induced sites in HIV gp120 correlate with the control of SHIV challenge in macaques vaccinated with subunit immunogens. *Proc. Natl. Acad. Sci. U. S. A.* 104:17477–17482. <http://dx.doi.org/10.1073/pnas.0707399104>.
- Joyce JG, Hurni WM, Bogusky MJ, Garsky VM, Liang X, Citron MP, Danzeisen RC, Miller MD, Shiver JW, Keller PM. 2002. Enhancement of α -helicity in the HIV-1 inhibitory peptide DPI78 leads to an increased affinity for human monoclonal antibody 2F5 but does not elicit neutralizing antibody responses in vitro. *J. Biol. Chem.* 277:45811–45820. <http://dx.doi.org/10.1074/jbc.M205862200>.
- Kim M, Qiao Z, Yu J, Montefiori D, Reinherz EL. 2007. Immunogenicity of recombinant human immunodeficiency virus type 1-like particles expressing gp41 derivatives in a pre-fusion state. *Vaccine* 25:5102–5114. <http://dx.doi.org/10.1016/j.vaccine.2006.09.071>.
- Cardoso RM, Zwick MB, Stanfield RL, Kunert R, Binley JM, Katinger H, Burton DR, Wilson IA. 2005. Broadly neutralizing anti-HIV antibody

- 4E10 recognizes a helical conformation of a highly conserved fusion-associated motif in gp41. *Immunity* 22:163–173. <http://dx.doi.org/10.1016/j.immuni.2004.12.011>.
23. Ofek G, Tang M, Sambor A, Katinger H, Mascola JR, Wyatt R, Kwong PD. 2004. Structure and mechanistic analysis of the anti-human immunodeficiency virus type 1 antibody 2F5 in complex with its gp41 epitope. *J. Virol.* 78:10724–10737. <http://dx.doi.org/10.1128/JVI.78.19.10724-10737.2004>.
 24. Saphire EO, Parren PW, Pantophlet R, Zwick MB, Morris GM, Rudd PM, Dwek RA, Stanfield RL, Burton DR, Wilson IA. 2001. Crystal structure of a neutralizing human IgG against HIV-1: a template for vaccine design. *Science* 293:1155–1159. <http://dx.doi.org/10.1126/science.1061692>.
 25. Stanfield RL, Gorny MK, Williams C, Zolla-Pazner S, Wilson IA. 2004. Structural rationale for the broad neutralization of HIV-1 by human monoclonal antibody 447-52D. *Structure (Camb.)* 12:193–204. <http://dx.doi.org/10.1016/j.str.2004.01.003>.
 26. Zhou T, Xu L, Dey B, Hessel AJ, Van Ryk D, Xiang SH, Yang X, Zhang MY, Zwick MB, Arthos J, Burton DR, Dimitrov DS, Sodroski J, Wyatt R, Nabel GJ, Kwong PD. 2007. Structural definition of a conserved neutralization epitope on HIV-1 gp120. *Nature* 445:732–737. <http://dx.doi.org/10.1038/nature05580>.
 27. Haynes BF, Fleming J, St Clair EW, Katinger H, Stiegler G, Kunert R, Robinson J, Scearce RM, Plonk K, Staats HF, Ortel TL, Liao HX, Alam SM. 2005. Cardiophilic polyspecific autoreactivity in two broadly neutralizing HIV-1 antibodies. *Science* 308:1906–1908. <http://dx.doi.org/10.1126/science.1111781>.
 28. Haynes BF, Moody MA, Verkoczy L, Kelsoe G, Alam SM. 2005. Antibody polyspecificity and neutralization of HIV-1: a hypothesis. *Hum. Antibodies* 14:59–67. <http://www.ncbi.nlm.nih.gov/pmc/article/PMC2673565>.
 29. Fernando K, Hu H, Ni H, Hoxie JA, Weissman D. 2007. Vaccine-delivered HIV envelope inhibits CD4+ T-cell activation, a mechanism for poor HIV vaccine responses. *Blood* 109:2538–2544. <http://dx.doi.org/10.1182/blood-2006-08-038661>.
 30. He B, Qiao X, Klasse PJ, Chiu A, Chadburn A, Knowles DM, Moore JP, Cerutti A. 2006. HIV-1 envelope triggers polyclonal IgG class switch recombination through a CD40-independent mechanism involving BAFF and C-type lectin receptors. *J. Immunol.* 176:3931–3941. <http://www.jimmunol.org/content/176/7/3931.long>.
 31. Shan M, Klasse PJ, Banerjee K, Dey AK, Iyer SPN, Dionisio R, Charles D, Campbell-Gardener L, Olson WC, Sanders RW, Moore JP. 2007. HIV-1 gp120 mannoses induce immunosuppressive responses from dendritic cells. *PLoS Pathog.* 3:e169. <http://dx.doi.org/10.1371/journal.ppat.0030169>.
 32. McMichael AJ, Haynes BF. 2012. Lessons learned from HIV-1 vaccine trials: new priorities and directions. *Nat. Immunol.* 13:423–427. <http://dx.doi.org/10.1038/ni.2264>.
 33. Liao H-X, Lynch R, Zhou T, Gao F, Alam SM, Boyd SD, Fire AZ, Roskin KM, Schramm CA, Zhang Z, Zhu J, Shapiro L, Comparative Sequencing Program NISC, Mullikin JC, Gnanakaran S, Hraber P, Wiehe K, Kelsoe G, Yang G, Xia SM, Montefiori DC, Parks R, Lloyd KE, Scearce RM, Soderberg KA, Cohen M, Kamanga G, Louder MK, Tran LM, Chen Y, Cai F, Chen S, Moquin S, Du X, Joyce MG, Srivatsan S, Zhang B, Zheng A, Shaw GM, Hahn BH, Kepler TB, Korber BT, Kwong PD, Mascola JR, Haynes BF. 2013. Co-evolution of a broadly neutralizing HIV-1 antibody and founder virus. *Nature* 496:469–476. <http://dx.doi.org/10.1038/nature12053>.
 34. Jardine J, Julien JP, Menis S, Ota T, Kalyuzhnyi O, McGuire A, Sok D, Huang PS, MacPherson S, Jones M, Nieuwma T, Mathison J, Baker D, Ward AB, Burton DR, Stamatatos L, Nemazee D, Wilson IA, Schief WR. 2013. Rational HIV immunogen design to target specific germline B cell receptors. *Science* 340:711–716. <http://dx.doi.org/10.1126/science.1234150>.
 35. Li M, Gao F, Mascola JR, Stamatatos L, Polonis VR, Koutsoukos M, Voss G, Goepfert P, Gilbert P, Greene KM, Bilska M, Kothe DL, Salazar-Gonzalez JF, Wei X, Decker JM, Hahn BH, Montefiori DC. 2005. Human immunodeficiency virus type 1 *env* clones from acute and early subtype B infections for standardized assessments of vaccine-elicited neutralizing antibodies. *J. Virol.* 79:10108–10125. <http://dx.doi.org/10.1128/JVI.79.16.10108-10125.2005>.
 36. Li M, Salazar-Gonzalez JF, Derdeyn CA, Morris L, Williamson C, Robinson JE, Decker JM, Li Y, Salazar MG, Polonis VR, Mlisana K, Karim SA, Hong K, Greene KM, Bilska M, Zhou J, Allen S, Chomka E, Mulenga J, Vwalika C, Gao F, Zhang M, Korber BT, Hunter E, Hahn BH, Montefiori DC. 2006. Genetic and neutralization properties of subtype C human immunodeficiency virus type 1 molecular *env* clones from acute and early heterosexually acquired infections in southern Africa. *J. Virol.* 80:11776–11790. <http://dx.doi.org/10.1128/JVI.01730-06>.
 37. Mascola JR, D'Souza P, Gilbert P, Hahn B, Haigwood NL, Morris L, Petropoulos CJ, Polonis VR, Sarzotti M, Montefiori DC. 2005. Recommendations for the design and use of standard virus panels to assess the neutralizing antibody response elicited by candidate human immunodeficiency virus type 1 vaccines. *J. Virol.* 79:10103–10107. <http://dx.doi.org/10.1128/JVI.79.16.10103-10107.2005>.
 38. Brown BK, Darden JM, Tovanabutra S, Oblander T, Frost J, Sanders-Buell E, de Souza MS, Bix DL, McCutchan FE, Polonis VR. 2005. Biologic and genetic characterization of a panel of 60 human immunodeficiency virus type 1 isolates, representing clades A, B, C, D, CRF01_AE, and CRF02_AG, for the development and assessment of candidate vaccines. *J. Virol.* 79:6089–6101. <http://dx.doi.org/10.1128/JVI.79.10.6089-6101.2005>.
 39. Simek MD, Rida W, Priddy FH, Pung P, Carrow E, Laufer DS, Lehrman JK, Boaz M, Tarragona-Fiol T, Miiro G, Birungi J, Pozniak A, McPhee DA, Manigart O, Karita E, Inwoley A, Jaoko W, Dehovitz J, Bekker LG, Pitisuttithum P, Paris R, Walker LM, Poignard P, Wrin T, Fast PE, Burton DR, Koff WC. 2009. Human immunodeficiency virus type 1 elite neutralizers: individuals with broad and potent neutralizing activity identified by using a high-throughput neutralization assay together with an analytical selection algorithm. *J. Virol.* 83:7337–7348. <http://dx.doi.org/10.1128/JVI.00110-09>.
 40. Wu X, Yang ZY, Li Y, Hogerkorp CM, Schief WR, Seaman MS, Zhou T, Schmidt SD, Wu L, Xu L, Longo NS, McKee K, O'Dell S, Louder MK, Wycuff DL, Feng Y, Nason M, Doria-Rose N, Connors M, Kwong PD, Roederer M, Wyatt RT, Nabel GJ, Mascola JR. 2010. Rational design of envelope identifies broadly neutralizing human monoclonal antibodies to HIV-1. *Science* 329:856–861. <http://dx.doi.org/10.1126/science.1187659>.
 41. Zhou T, Georgiev I, Wu X, Yang ZY, Dai K, Finzi A, Kwon YD, Scheid JF, Shi W, Xu L, Yang Y, Zhu J, Nussenzweig MC, Sodroski J, Shapiro L, Nabel GJ, Mascola JR, Kwong PD. 2010. Structural basis for broad and potent neutralization of HIV-1 by antibody VRC01. *Science* 329:811–817. <http://dx.doi.org/10.1126/science.1192819>.
 42. Bonsignori M, Montefiori DC, Wu X, Chen X, Hwang KK, Tsao CY, Kozink DM, Parks RJ, Tomaras GD, Crump JA, Kapiga SH, Sam NE, Kwong PD, Kepler TB, Liao HX, Mascola R, Haynes BF. 2012. Two distinct broadly neutralizing antibody specificities of different clonal lineages in a single HIV-1-infected donor: implications for vaccine design. *J. Virol.* 86:4688–4692. <http://dx.doi.org/10.1128/JVI.07163-11>.
 43. Wu X, Zhou T, Zhu J, Zhang B, Georgiev I, Wang C, Chen X, Longo NS, Louder M, McKee K, O'Dell S, Perfetto S, Schmidt SD, Shi W, Wu L, Yang Y, Yang ZY, Yang Z, Zhang Z, Bonsignori M, Crump JA, Kapiga SH, Sam NE, Haynes BF, Simek M, Burton DR, Koff WC, Doria-Rose NA, Connors M, Comparative Sequencing Program NISC, Mullikin JC, Nabel GJ, Roederer M, Shapiro L, Kwong PD, Mascola JR. 2011. Focused evolution of HIV-1 neutralizing antibodies revealed by structures and deep sequencing. *Science* 333:1593–1602. <http://dx.doi.org/10.1126/science.1207532>.
 44. Corti D, Langedijk JP, Hinz A, Seaman MS, Vanzetta F, Fernandez-Rodriguez BM, Silacci C, Pinna D, Jarrossay D, Balla-Jhaghoorsingh S, Willems B, Zekveld MJ, Dreja H, O'Sullivan E, Pade C, Orkin C, Jeffs SA, Montefiori DC, Davis D, Weissenhorn W, McKnight A, Heeney JL, Sallusto F, Sattentau QJ, Weiss RA, Lanzavecchia A. 2010. Analysis of memory B cell responses and isolation of novel monoclonal antibodies with neutralizing breadth from HIV-1-infected individuals. *PLoS One* 5:e8805. <http://dx.doi.org/10.1371/journal.pone.0008805>.
 45. Burton DR, Pyati J, Koduri R, Sharp SJ, Thornton GB, Parren PW, Sawyer LS, Hendry RM, Dunlop N, Nara PL, et al. 1994. Efficient neutralization of primary isolates of HIV-1 by a recombinant human monoclonal antibody. *Science* 266:1024–1027. <http://dx.doi.org/10.1126/science.7973652>.
 46. Walker LM, Phogat SK, Chan-Hui PY, Wagner D, Phung P, Goss JL, Wrin T, Simek MD, Fling S, Mitcham JL, Lehrman JK, Priddy FH, Olsen OA, Frey SM, Hammond PW, Kaminsky S, Zamb T, Moyle M, Koff WC, Poignard P, Burton DR. 2009. Broad and potent neutralizing antibodies from an African donor reveal a new HIV-1 vaccine target. *Science* 326:285–289. <http://dx.doi.org/10.1126/science.1178746>.
 47. Bonsignori M, Hwang K-K, Chen X, Tsao C-Y, Morris L, Gray E, Marshall DJ, Crump JA, Kapiga SH, Sam NE, Sinangil F, Pancera M,

- Yongping Y, Zhang B, Zhu J, Kwong PD, O'Dell S, Mascola JR, Wu L, Nabel GJ, Phogat S, Seaman MS, Whitesides JF, Moody MA, Kelsoe G, Yang X, Sodroski J, Shaw GM, Montefiori DC, Kepler TB, Tomaras GD, Alam SM, Liao HX, Haynes BF. 2011. Analysis of a clonal lineage of HIV-1 envelope V2/V3 conformational epitope-specific broadly neutralizing antibodies and their inferred unmutated common ancestors. *J. Virol.* 85:9998–10009. <http://dx.doi.org/10.1128/JVI.05045-11>.
48. Walker LM, Huber M, Doores KJ, Falkowska E, Pejchal R, Julien J-P, Wang S-K, Ramos A, Chan-Hui PY, Moyle M, Mitcham JL, Hammond PW, Olsen OA, Phung P, Fling S, Wong C-H, Phogat S, Wrinn T, Simek MD, Protocol G Principal Investigators, Koff WC, Wilson IA, Burton DR, Poignard P. 2011. Broad neutralization coverage of HIV by multiple highly potent antibodies. *Nature* 477:466–470. <http://dx.doi.org/10.1038/nature10373>.
49. Calarese DA, Scanlan CN, Zwick MB, Deechongkit S, Mimura Y, Kunert R, Zhu P, Wormald MR, Stanfield RL, Roux KH, Kelly JW, Rudd PM, Dwek RA, Katinger H, Burton DR, Wilson IA. 2003. Antibody domain exchange is an immunologic solution to carbohydrate cluster recognition. *Science* 300:2065–2071. <http://dx.doi.org/10.1126/science.1083182>.
50. Zwick MB, Labrijn AF, Wang M, Spenlehauer C, Saphire EO, Binley JM, Moore JP, Stiegler G, Katinger H, Burton DR, Parren PWHI. 2001. Broadly neutralizing antibodies targeted to the membrane-proximal external region of human immunodeficiency virus type 1 glycoprotein gp41. *J. Virol.* 75:10892–10905. <http://dx.doi.org/10.1128/JVI.75.22.10892-10905.2001>.
51. Nyambi PN, Gorny MK, Bastiani L, van der Groen G, Williams C, Zolla-Pazner S. 1998. Mapping of epitopes exposed on intact human immunodeficiency virus type 1 (HIV-1) virions: a new strategy for studying the immunologic relatedness of HIV-1. *J. Virol.* 72:9384–9391.
52. Jeffs SA, Gorny MK, Williams C, Revesz K, Volsky B, Burda S, Wang XH, Bandres J, Zolla-Pazner S, Holmes H. 2001. Characterization of human monoclonal antibodies selected with a hypervariable loop-deleted recombinant HIV-1 (IIIB) gp120. *Immunol. Lett.* 79:209–213. [http://dx.doi.org/10.1016/S0165-2478\(01\)00289-9](http://dx.doi.org/10.1016/S0165-2478(01)00289-9).
53. Zolla-Pazner S, O'Leary J, Burda S, Gorny MK, Kim M, Mascola J, McCutchan FE. 1995. Serotyping of primary human immunodeficiency virus type 1 isolates from diverse geographic locations by flow cytometry. *J. Virol.* 69:3807–3815.
54. Gorny MK, Williams C, Volsky B, Revesz K, Cohen S, Polonis VR, Honnen WJ, Kayman SC, Krachmarov CP, Pinter A, Zolla-Pazner S. 2002. Human monoclonal antibodies specific for conformation-sensitive epitopes of V3 neutralize HIV-1 primary isolates from various clades. *J. Virol.* 76:9035–9045. <http://dx.doi.org/10.1128/JVI.76.18.9035-9045.2002>.
55. Gorny MK, Revesz K, Williams C, Volsky B, Louder MK, Anyangwe CA, Krachmarov CP, Kayman SC, Pinter A, Nadas A, Nyambi PN, Mascola JR, Zolla-Pazner S. 2004. The V3 loop is accessible on the surface of most human immunodeficiency virus type 1 primary isolates and serves as a neutralization epitope. *J. Virol.* 78:2394–2404. <http://dx.doi.org/10.1128/JVI.78.5.2394-2404.2004>.
56. Gorny MK, Williams C, Volsky B, Revesz K, Wang XH, Burda S, Kimura T, Koning FA, Nadas A, Anyangwe C, Nyambi P, Krachmarov C, Pinter A, Zolla-Pazner S. 2006. Cross-clade neutralizing activity of human anti-V3 monoclonal antibodies derived from the cells of individuals infected with non-B clades of HIV-1. *J. Virol.* 80:6865–6872. <http://dx.doi.org/10.1128/JVI.02202-05>.
57. Gorny MK, Wang XH, Williams C, Volsky B, Revesz K, Witover B, Burda S, Urbanski M, Nyambi P, Krachmarov C, Pinter A, Zolla-Pazner S, Nadas A. 2009. Preferential use of the VH5-51 gene segment by the human immune response to code for antibodies against the V3 domain of HIV-1. *Mol. Immunol.* 46:917–926. <http://dx.doi.org/10.1016/j.molimm.2008.09.005>.
58. Gorny MK, Xu J-Y, Karwowska S, Buchbinder A, Zolla-Pazner S. 1993. Repertoire of neutralizing human monoclonal antibodies specific for the V3 domain of HIV-1 gp120. *J. Immunol.* 150:635–643.
59. Gorny MK, VanCott TC, Hioe C, Israel Z, Michael NL, Conley AJ, Williams C, Kessler JA, II, Chigurupati P, Burda S, Zolla-Pazner S. 1997. Human monoclonal antibodies to the V3 loop of HIV-1 with intra- and interclade cross-reactivity. *J. Immunol.* 159:5114–5122.
60. Gorny MK, VanCott TC, Williams C, Revesz K, Zolla-Pazner S. 2000. Effects of oligomerization on the epitopes of the human immunodeficiency virus type 1 envelope glycoproteins. *Virology* 267:220–228. <http://dx.doi.org/10.1006/viro.1999.0095>.
61. Nyambi PN, Mbah HA, Burda S, Williams C, Gorny MK, Nadas A, Zolla-Pazner S. 2000. Conserved and exposed epitopes on intact, native, primary human immunodeficiency virus type 1 virions of group M. *J. Virol.* 74:7096–7107. <http://dx.doi.org/10.1128/JVI.74.15.7096-7107.2000>.
62. Gorny MK, Moore JP, Conley AJ, Karwowska S, Sodroski J, Williams C, Burda S, Boots LJ, Zolla-Pazner S. 1994. Human anti-V2 monoclonal antibody that neutralizes primary but not laboratory isolates of HIV-1. *J. Virol.* 68:8312–8320.
63. Gorny MK, Pan R, Williams C, Wang XH, Volsky B, O'Neal T, Spurrier B, Sampson JM, Li L, Seaman MS, Kong XP, Zolla-Pazner S. 2012. Functional and immunochemical cross-reactivity of V2-specific monoclonal antibodies from human immunodeficiency virus type 1-infected individuals. *Virology* 427:198–207. <http://dx.doi.org/10.1016/j.viro.2012.02.003>.
64. Xu J-Y, Gorny MK, Palker T, Karwowska S, Zolla-Pazner S. 1991. Epitope mapping of two immunodominant domains of gp41, the transmembrane protein of human immunodeficiency virus type 1, using ten human monoclonal antibodies. *J. Virol.* 65:4832–4838.
65. Gorny MK, Gianakakos V, Sharpe S, Zolla-Pazner S. 1989. Generation of human monoclonal antibodies to HIV. *Proc. Natl. Acad. Sci. U. S. A.* 86:1624–1628. <http://dx.doi.org/10.1073/pnas.86.5.1624>.
66. Gigler A, Dorsch S, Hemauer A, Williams C, Kim S, Young NS, Zolla-Pazner S, Wolf H, Gorny MK, Modrow S. 1999. Generation of neutralizing human monoclonal antibodies against parvovirus B19 proteins. *J. Virol.* 73:1974–1979.
67. Edmonds TG, Ding H, Yuan X, Wei Q, Smith KS, Conway JA, Wiczorek L, Brown B, Polonis V, West JT, Montefiori DC, Kappes JC, Ochsenbauer C. 2010. Replication competent molecular clones of HIV-1 expressing Renilla luciferase facilitate the analysis of antibody inhibition in PBMC. *Virology* 408:1–13. <http://dx.doi.org/10.1016/j.viro.2010.08.028>.
68. Montefiori DC. 2009. Measuring HIV neutralization in a luciferase reporter gene assay. *Methods Mol. Biol.* 485:395–405. http://dx.doi.org/10.1007/978-1-59745-170-3_26.
69. McLinden RJ, LaBranche CC, Chenine A-L, Polonis VR, Eller M, Ochsenbauer C, Kappes JC, Perfetto S, Montefiori DC, Michael NL, Kim JH. 2013. Detection of HIV-1 neutralizing antibodies in a human CD4+/CCR5+/CXCR4+ T-lymphoblastoid cell assay system. *PLoS One* 8:e77756. <http://dx.doi.org/10.1371/journal.pone.0077756>.
70. Sarzotti-Kelsoe M, Bailer RT, Turk E, Lin CL, Bilska M, Greene KM, Gao H, Todd CA, Ozaki DA, Seaman MS, Mascola JR, Montefiori DC. 1 December 2013. Optimization and validation of the TZM-bl assay for standardized assessments of neutralizing antibodies against HIV-1. *J. Immunol. Methods* <http://dx.doi.org/10.1016/j.jim.2013.11.022>.
71. Sarzotti-Kelsoe M, Daniell X, Todd CA, Bilska M, Martelli A, LaBranche C, Perez LG, Ochsenbauer C, Kappes JC, Rountree W, Denny TN, Montefiori DC. Optimization and validation of a neutralizing antibody assay for HIV-1 in A3R5 cells. *J. Immunol. Methods*, in press.
72. Yu X, Gilbert PB, Hioe CE, Zolla-Pazner S, Self SG. 2012. Statistical approaches to analyzing HIV-1 neutralizing antibody assay data. *Stat. Biopharm. Res.* 4:1–13. <http://dx.doi.org/10.1080/19466315.2011.633860>.
73. Huang Y, Gilbert PB, Montefiori DC, Self SG. 2009. Simultaneous evaluation of the magnitude and breadth of a left- and right-censored multivariate response, with application to HIV vaccine development. *Stat. Biopharm. Res.* 1:81–91. <http://dx.doi.org/10.1198/sbr.2009.0008>.
74. Tibshirani R. 1996. Regression shrinkage and selection via the lasso. *J. R. Stat. Soc. Ser. B.* 58:267–288.
75. Yuan M, Lin Y. 2006. Model selection and estimation in regression with grouped variables. *J. R. Stat. Soc. Ser. B.* 68:49–67. <http://dx.doi.org/10.1111/j.1467-9868.2005.00532.x>.
76. Gottschalk PG, Dunn JR. 2005. The five-parameter logistic: a characterization and comparison with the four-parameter logistic. *Anal. Biochem.* 343:54–65. <http://dx.doi.org/10.1016/j.ab.2005.04.035>.
77. Ritz C, Streibig JC. 2005. Bioassay analysis using R. *J. Stat. Software* 12(5). <http://www.jstatsoft.org/v12/i05/paper>.
78. West AP, Scharf L, Horwitz J, Klein F, Nussenzweig MC, Bjorkman PJ. 2013. Computational analysis of anti-HIV-1 antibody neutralization panel data to identify potential functional epitope residues. *Proc. Natl. Acad. Sci. U. S. A.* 110:10598–10603. <http://dx.doi.org/10.1073/pnas.1309215110>.
79. Balla-Jhaghoorsingh SS, Corti D, Heyndrickx L, Willems E, Vereecken K, Davis D, Vanham G. 2013. The N276 glycosylation site is required for HIV-1 neutralization by the CD4 binding site specific HJ16 monoclonal

- antibody. *PLoS One* 8:e68863. <http://dx.doi.org/10.1371/journal.pone.0068863>.
80. McLellan JS, Pancera M, Carrico C, Gorman J, Julien JP, Khayat R, Louder R, Pejchal R, Sastry M, Dai K, O'Dell S, Patel N, Shahzad-ul Hussan S, Yang Y, Zhang B, Zhou T, Zhu J, Boyington JC, Chuang GY, Diwanji D, Georgiev I, Kwon YD, Lee D, Louder MK, Moquin S, Schmidt SD, Yang ZY, Bonsignori M, Crump JA, Kapiga SH, Sam NE, Haynes BF, Burton DR, Koff WC, Walker LM, Phogat S, Wyatt R, Orwenyo J, Wang LX, Arthos J, Bewley CA, Mascola JR, Nabel GJ, Schief WR, Ward AB, Wilson IA, Kwong PD. 2011. Structure of HIV-1 gp120 V1/V2 domain with broadly neutralizing antibody PG9. *Nature* 480:336–343. <http://dx.doi.org/10.1038/nature10696>.
 81. West AP, Jr, Diskin R, Nussenzweig MC, Bjorkman PJ. 2012. Structural basis for germ-line gene usage of a potent class of antibodies targeting the CD4-binding site of HIV-1 gp120. *Proc. Natl. Acad. Sci. U. S. A.* 109: E2083–E2090. <http://dx.doi.org/10.1073/pnas.1208984109>.
 82. Li Y, O'Dell S, Walker LM, Wu X, Guenaga J, Feng Y, Schmidt SD, McKee K, Louder MK, Ledgerwood JE, Graham BS, Haynes BF, Burton DR, Wyatt RT, Mascola JR. 2011. Mechanism of neutralization by the broadly neutralizing HIV-1 monoclonal antibody VRC01. *J. Virol.* 85: 8954–8967. <http://dx.doi.org/10.1128/JVI.00754-11>.
 83. Hraber P, Seaman MS, Bailer RT, Mascola JR, Montefiori DC, Korber BT. 2014. Prevalence of broadly neutralizing antibody responses during chronic HIV-1 infection. *AIDS* 28:163–169.
 84. Binley J, Wrin T, Korber B, Zwick M, Wang M, Chappey C, Stiegler G, Kunert R, Zolla-Pazner S, Katinger H, Petropoulos C, Burton D. 2004. Comprehensive cross-subtype neutralization analysis of a panel of anti-human immunodeficiency virus type 1 monoclonal antibodies. *J. Virol.* 78:13232–13252. <http://dx.doi.org/10.1128/JVI.78.23.13232-13252.2004>.
 85. Montefiori DC, Karnasuta C, Huang Y, Ahmed H, Gilbert P, de Souza MS, McLinden R, Tovanabutra S, Laurence-Chenine A, Sanders-Buell E, Moody MA, Bonsignori M, Ochsenbauer C, Kappes J, Tang H, Greene K, Gao H, LaBranche CC, Andrews C, Polonis VR, Rerks-Ngarm S, Pitisuttithum P, Nitayaphan S, Kaewkungwal J, Self SG, Berman PW, Francis D, Sinangil F, Lee C, Tartaglia J, Robb ML, Haynes BF, Michael NL, Kim JH. 2012. Magnitude and breadth of the neutralizing antibody response in the RV144 and Vax003 HIV-1 vaccine efficacy trials. *J. Infect. Dis.* 206:431–441. <http://dx.doi.org/10.1093/infdis/jis367>.